学位論文

新規モノクローナル抗体の作製に
あたってのエピトープの選択と
抗体の機能に関する研究

舟橋　真一

目次

【様　式】

博士論文要旨

氏名　舟　橋　　真　一

論文題名　新規モノクローナル抗体の作製にあたっての
エピトープの選択と抗体の機能に関する研究

主査　島田　章則

副査　栗林　尚志

荻原　喜久美

モノクローナル抗体は、その特異性から分子生物学的ならびに病理組織学的な分子の検出・解析に威力を発揮するとともに、抗体の持つ機能との組み合わせにより分子標的治療にも広く活用されている。本研究では二つのモノクローナル抗体の取得について報告する。一報は幹細胞の分子生物学的・病理組織学的研究への展開を目指したモノクローナル抗体の取得に関する研究であり、もう一報は、そこから得られたナレッジを活用した抗体創薬に向けたモノクローナル抗体の取得に関する研究である。

Ⅰ. LGR6 (Leucine-rich repeat (LRR)-containing G protein-coupled receptor) に対するモノクローナル抗体の作製とその性状

LGR6 は G タンパク質共役受容体 (GPCR) の一つで、ロイシン・リッチ・リピートを含む GPCR(LGR)ファミリーのメンバーである。LGR6 は、LGR4, 5 とともに LGR のサブファミリーを形成し、これらの分子で最も研究が進んでいるのは LGR5 である。LGR5 は小腸、胃、皮膚の幹細胞、および大腸癌幹細胞のマーカーとして知られており、我々は先の研究で LGR5 の発現が大腸癌幹細胞の増殖と静止状態を区別する分子病理学的マーカーであることを報告した。今回研究を進めた LGR6 も、genetic lineage tracing の解析から原始の皮膚の幹細胞マーカーとして報告されている。しかし、LGR6 の組織学的な発現情報や LGR6 陽性細胞の機能・役割については、特異的な抗体が得られていないためにいまだ詳細に解明されていない。我々が抗 LGR5 抗体を取得する際に経験した困難さから LGR6 特異的抗体が得られていないのは、このサブファミリーに特徴的なタンパクの構造に起因するものと考えられた。すなわち、LGR サブファミリーは N 末端に馬蹄形をした 500 アミノ酸からなるロイシン・リッチ・リピート領域を有し、この複雑な立体構造を維持した免疫抗原を調製することが難しいこと、また、ロイシン・リッチ・リピート領域を含めサブファミリー分子間の相同性が高く、ファミリー分子に交差しない特異的抗体の取得が難しいことが考えられた。

そこで我々はこれらの課題を克服するために、DNA 免疫法による LGR6 特異的抗体の作製を試みた。DNA 免疫法では、金粒子にコーティングした発現プラスミドを GeneGun によって高圧でマウスの腹部に接種し、発現プラスミドが導入された細胞ではタンパク質が産生され、これらのタンパク質は立体構造を維持した状態で細胞膜上に提示され、免疫抗原としてマウスでの抗体産生を誘導することができる。LGR6 発現プラスミドを DNA 免疫法で Balb/c マウスに導入した結果、LGR6

に対する液性免疫が誘導され、LGR6 に対する抗体が産生された。

LGR6 に対する抗体価が上昇したマウスに対し、さらに LGR6 に対する免疫を亢進させるためにブースト免疫として LGR6 タンパク質を高発現した細胞株の細胞免疫を実施した。LGR ファミリーを含む GPCR は一般に高発現株を取得することが難しいとされているが、我々は先の抗 LGR5 抗体取得の際に LGR5 を高発現させる方法としてマウス ProB 細胞株である Ba/F3 株を使用することが有効であることを経験していた。Ba/F3 株は目的の遺伝子を発現する細胞株の樹立にあまり広く利用されていない親株であるが、浮遊細胞のためフローサイトメトリー解析において細胞の調整が容易であり、また細胞の増殖が速いことから細胞株の樹立を早期に実現できるメリットがある。また、Ba/F3 株は Balb/c マウスに由来する細胞株であり、Balb/c マウスへ免疫する際には Ba/F3 株で発現される抗原のみが外来抗原と認識される。そこで、LGR6 高発現 Ba/F3 株を樹立し、細胞免疫を施すことで特異的な免疫増強による抗体価上昇を誘導し、抗 LGR6 モノクローナル抗体を取得することができた。

取得された抗体については、以下の流れで特性と機能の解析を行った。

1. LGR6 特異的抗体は、フローサイトメトリーを用いて細胞外領域への結合の有無でエピトープ分類を行い、N 末端の細胞外領域（N-ECD）を認識する抗体と 7 回膜貫通領域(7TM)の細胞外ループを認識する抗体のエピトープを確認した。その結果、N-ECD を認識する抗体２クローンと 7TM を認識する抗体１クローンを取得した。
2. LGR6 特異的抗体による LGR6 とリガンド RSPO-1 との結合阻害活性を解析した。RSPO-1 の LGR6 への結合を検出するため、タグ付きの組換えタンパク質の RSPO-1 を準備し、タグに対する抗体で検出するアッセイ系を構築した。反応系に加えた抗 LGR6 抗体の濃度依存的な結合阻害を評価した。その結果、43A6,

43D10の二つのクローンはLGR6とリガンドRSPO-1との結合を阻害することが明らかとなった。

DNA免疫と細胞免疫の二つの方法を組み合わせることによって、LGR6に特異的であるとともに、リガンドとレセプターの結合を阻害する中和活性のある抗体の取得にも成功した。これらの成果は、LGR6の立体構造を維持したタンパク質を免疫抗原として用いたことと、立体構造の維持によりリガンドの結合部位が保存されたという、免疫手法の選択・工夫がもたらしたものと考える。今回取得した抗体は、LGR6陽性細胞の役割・機能の解明など新たな幹細胞生物学の進展に貢献できるものと考える。

Ⅱ.扁平上皮癌への創薬応用を目指した天疱瘡作用の誘発しない抗デスモグレイン３ (Desmoglein 3 (DSG3))抗体の作製

近年、癌を標的としたモノクローナル抗体が分子標的治療薬として利用されてきている。抗体をベースとした創薬の特徴は、抗体の特異性と、中和活性、抗体依存的な細胞傷害活性（ADCC)、補体依存的な細胞傷害活性（CDC）といった抗体の機能の組み合わせにより癌細胞を死滅させることである。

癌に対する抗体創薬の新規標的分子は、遺伝子発現の多寡から候補遺伝子を絞り込む遺伝子発現解析と、その遺伝子から発現されるタンパク質の組織分布や細胞膜に位置しているかといった細胞内分布を解析する病理解析の両面から評価される。これらの解析から、我々はDSG3を重層扁平上皮癌に対する有望な標的分子として見出した。DSG3は一回膜貫通タンパク質で他のカドヘリン分子であるDSG1とともにデスモソームを形成し、重層扁平上皮組織での細胞間結合に寄与している。

抗 DSG3 自己抗体は皮膚粘膜の水疱を特徴とする自己免疫疾患の一つである天疱瘡の原因となることが知られている。DSG3 を標的とする創薬を進めるためには、天疱瘡様病変の誘発を回避し、かつ、重層扁平上皮癌に対して薬理作用を発揮しなければならない。これまでの研究より天疱瘡を引き起こす病原性の自己抗体は、Ca^{2+}依存的な構造をとる DSG3 を認識すること、自己抗体が認識する領域が N 末端の接着界面に存在することが報告されている。これらの知見より、Ca^{2+}非依存的に DSG3 に結合する抗体を取得することで副作用を回避した治療用抗体を取得できるものと仮説を立てた。

そこで、各種スクリーニング系を駆使し、目的とする特徴を有する抗体の取得を試みた。スクリーニング系では、DSG3 が生体内で本来形成している構造に近いタンパク質を準備し、エピトープの分類による抗体の選別を行った。抗マウス DSG3 抗体のスクリーニング過程を以下に示す。

1. マウス DSG3 に結合する抗体をフローサイトメトリーによりスクリーニングした。34 個のマウス DSG3 結合抗体を取得した。
2. 癌細胞の死滅誘導方法として ADCC を薬理作用に持つ抗体 12 クローンを選抜した。マウスの ADCC 活性を測定する安定したアッセイ系がないため、ヒト NK92 細胞を遺伝子工学的に改変した細胞株を用いたスクリーニング系を考案し、マウスとヒトの FcRγⅢa 融合タンパク質を発現させることによって NK 細胞によるマウス抗体の ADCC 活性を測定できる系が構築できた。
3. 抗体によって DSG3 の Ca^{2+} 依存的構造が認識されるかどうかを Ca^{2+}のキレート剤である EDTA 存在下でフローサイトメトリーを用いて評価した。3 クローンが Ca^{2+}非依存的に DSG3 に結合する抗体であった。そのうち最も結合アフィニティーの高いクローン 18-1 を選定した。
4. 天疱瘡様病変を誘発する抗体は、細胞間の接着を分離する活性を有していることからマウス由来の皮膚細胞シートを用いたスクリーニング方法により抗

体が細胞の接着機能を阻害する能力があるかどうかを判断した。クローン18-1は細胞間接着の分離活性は有していなかった。

上記スクリーニング系でマウス DSG3 に対する副作用の回避が可能と考えられる抗体18-1を取得できた。次に、*in vivo*モデルでの解析として、DSG3を発現するマウス肺癌細胞株LC12を移植したマウスによる抗腫瘍効果を評価した。その結果、抗マウスDSG3抗体18-1の投与による天疱瘡様病変はみられず、LC12癌組織の退縮が観察された。副作用を誘導するエピトープを避け、ADCCを誘導するエピトープを選択することにより DSG3 に対する創薬抗体の作製が可能であることがマウスモデル系で示された。

次に、同様のスクリーニングフローを用い、ヒトDSG3に対し天疱瘡様病変の誘発作用がなく、高いADCC作用を持つ抗体DF366を取得した。種々のヒト重層扁平上皮癌担癌モデルでの抗ヒトDSG3抗体DF366の抗腫瘍効果を確認し、抗体医薬としての可能性を示した。

Ⅲ. 総括

二つの解析から目的のエピトープを持つ抗体を作製するための要点は次にあげる二点となる。一つは、免疫やスクリーニングに用いるタンパク質は機能的に天然の構造を持ったものを利用することであり、もう一つは、エピトープを分類することで適切な抗体の機能を付加できるような抗体の分類をすることである。これらのステップは目的の機能を持った抗体を同定・取得する有用なアプローチを提供するものである。

現在、抗体創薬標的分子は枯渇している。今回、医薬品とするためには不都合な作用のある抗原であってもエピトープの選択次第で新しい創薬への展開が可能となることを示唆した。この研究は、分子標的薬としての抗体創薬の標的分子の選択可能性を広げるものであり、今後の抗体医薬品の研究開発に貢献するものと考える。

本論文の一部は以下に公表した。

1. **Generation and characterization of monoclonal antibodies against human LGR6.**
   Funahashi SI, Suzuki Y, Nakano K, Kawai S, Suzuki M.
   "This is a pre-copyedited, author-produced version of an article accepted for publication in The Journal of Biochemistry following peer review. The version of record [The Journal of Biochemistry (2017) 161(4): 361-368] is available online at: https://doi.org/10.1093/jb/mvw077"

2. **Generation of an anti-desmoglein 3 antibody without pathogenic activity of pemphigus vulgaris for therapeutic application to squamous cell carcinoma**
   Funahashi SI, Kawai S, Fujii E, Taniguchi K, Nakano K, Ishikawa S, Aburatani H, Suzuki M.
   The Journal of Biochemistry (2018) 164(6): 471-481.
   https://doi.org/10.1093/jb/mvy074

A study on the effectiveness of combinationing epitope selection and antibody function for the generation of novel monoclonal antibodies

Abstract:

Monoclonal antibodies are considered powerful tools for molecular biological or histopathological detection and analysis of a molecule due to their specificity, and they are also widely utilized for molecular targeted therapy by combining their specificity and functionality.

In the current research the process of the generation of two unique monoclonal antibodies was studied. With the first antibody, the process of obtaining a monoclonal antibody aimed for application to molecular biological or histopathological analysis in stem cell research is studied, and for the second, the knowledge obtained in the process for the first antibody is applied for development of an antibody therapy.

I. Generation and characterization of monoclonal antibodies against human LGR6 (Leucine-rich repeat (LRR)-containing G protein-coupled receptor)

LGR6 is a G protein-coupled receptor (GPCR) and a member of the LRR containing GPCR (LGR) family. LGR4, 5 and 6 belong to the same subfamily and one of the best studied is LGR5. LGR5 is known as a marker of intestinal, gastric, skin and also colon cancer stem cells. We previously reported that LGR5 expression could be used as a molecular pathological marker to distinguish the states of proliferating and quiescent cancer stem cells. LGR6 is also known as a marker for primitive epidermal stem cells from genetic lineage tracing analysis. However, information concerning its histological expression, cellular functions and physiological roles of is scarce due to the lack of a specific antibody. From our previous experience in obtaining an LGR5 antibody, we judged that we would face similar difficulties with an LGR6 antibody because of the complex structure of LGR proteins. LGRs have about 500 amino acids' length of LRR region with a horseshoe structure in the N-terminus and this complex tertiary structural feature makes it a challenge to prepare immunogen. In addition, it is difficult to obtain antibodies that do not cross-reactive to other LGRs because of high homology between subfamily molecules with the LRR region.

Thus we attempted to generate a LGR6-specific antibody by DNA immunization to overcome these problems. For DNA immunization gold particles coated with plasmids expressing the molecule of interest are prepared. The particles are injected into the abdominal skin of mice with a

high pressured GeneGun inducing the protein encoded in the plasmids. The protein is displayed on the plasma membrane with a native tertiary structure, and was thought to be a robust immunogen for induction of humoral antibody production in mice. By introducing a plasmid expressing the LGR6 gene in Balb/c mice we succeeded in inducing a humoral immune response to obtain antibodies against LGR6.

Furthermore, to enhance immunity against LGR6, we additionally injected a cell line overexpressing LGR6 as a boosting immunogen into the mice that were immunized by the plasmids with high titers of anti-LGR6 antibodies. Although, it is generally a challenge to obtain a stable cell line overexpressing GPCRs including the LGR family proteins, we found in our experience with LGR5 that it is effective to use the mouse proB cell, Ba/F3 cell. Ba/F3 is not frequently used for the establishment of cell lines with specific gene expression. However this cell line is a floating cell that can be analyzed easily by flow cytometry and because of its rapid growth, the establishment of a cell line can be accomplished in a short time. As Ba/F3 is derived from Balb/c mice, human antigens expressed in Ba/F3 cells, can be recognized specifically as a foreign antigen when injected into Balb/c mice. By this method, LGR6-specific immunity was augmented, making it easier to obtain monoclonal antibodies against LGR6.

According to the following flow, the characteristics and functions of the monoclonal antibodies against LGR6 obtained with the above methods were analyzed.

1. Epitope classification was carried out by identifying binders to the N-terminal extracellular domain (N-ECD) or 7-pass transmembrane domain (7TM) of LGR6 by flow cytometry. As a result, we obtained three clones, 43A6 and 43D10, with an epitope against N-ECD and 43A25 against 7TM.
2. The inhibitory activity of the antibodies against ligand binding to LGR6 was evaluated. It is well known that RSPO1 is a ligand that binds to the N-ECD of LGR6. Recombinant RSPO1 with a myc-His tag was prepared and an assay system for detection of RSPO1-bindig to LGR6 was established with an anti-myc tag antibody. Binding inhibition dependent on antibody concentration was evaluated. As a result, 2 clones, 43A6 and 43D10, were found to inhibit binding of ligand to LGR6. On the other hand, 43A25 did not inhibit RSPO1-binding.

The key to our success with the LGR6 antibodies was thought to be the selection of the immunization method of combining DNA and cell immunization which enabled immunization with an immunogen preserving the native tertiary structure of the ligand binding site of LGR6.

Utilizing our unique antibodies may lead to understanding the role and function of LRG6-positive cells, and we anticipate that this may contribute to the progress in stem cell research.

II. Generation of anti-desmoglein 3 (DSG3) antibody without pathogenic activity of pemphigus vulgaris for therapeutic application to squamous cell carcinoma

In the second report, therapeutic application of an anti-DSG3 monoclonal antibody is studied. Cancer-targeted monoclonal antibodies are frequently utilized in cancer therapy. The advantage of antibody-based therapeutics is their specificity and functionality such as neutralization, antibody-dependent cell-mediated cytotoxicity (ADCC), or complement-dependent cytotoxicity (CDC), by which the antibody can eliminate cancer cells. Many therapeutic antibodies against cancer have been launched and there have been great benefits for the therapeutic modality in the oncology field.

Prior to our second study, candidate genes with high gene expression levels in tumor tissues compared to normal tissues were selected in order to discover a novel drug target for antibody therapy in cancer patients The tissue distribution of the gene product and their subcellular localization to the cell membrane in tumor tissues was studied to confirm the protein expression. By this process we found that DSG3 is a promising target for squamous cell carcinoma. DSG3 is a one-pass transmembrane protein and forms desmosomes along with another desmosomal cadherin, DSG1, and contributes to cell-cell adhesion in stratified squamous tissues.

It is well known that anti-DSG3 autoantibodies cause PV, an autoimmune disease characterized by cutaneous and mucosal blistering. To successfully target DSG3 for therapy, it is necessary to avoid PV-like effects and exert pharmacological action against squamous carcinoma cells. It is

reported that pathogenic autoantibodies which induce PV recognizes a Ca^{2+}-dependent structure of DSG3 and the region bound by DSG3-autoanibodies is located in the N-terminal adhesive interface. From these findings, we hypothesized that a therapeutic antibody with no severe side effects could be generated by obtaining antibodies that bind DSG3 in Ca^{2+}-independent manner.

Thus, we attempted to obtain such an antibody by using several screening systems. In the screening system we prepared proteins mimicking the native conformation of DSG3 and selected antibodies by epitope classification. Our screening process is shown below.

1. Antibodies with the ability to bind mouse DSG3 were selected by flow cytometry. 34 clones were found to bind mouse DSG3.
2. We selected ADCC as the pharmacological action of antibodies, and 12 antibodies with ADCC function through the following screening system. To construct a stable assay for ADCC activity, we designed a screening system using genetically engineered NK cells. We established an ADCC assay system with human NK92 cells expressing a chimeric protein with the ECD of mouse FcγRIIIa fused to the human transmembrane and cytoplasmic domain of FcγRIIIa.
3. Recognition of the Ca^{2+} dependent structure of DSG3 was evaluated by flow cytometry under the presence of an EDTA, a Ca^{2+} chelator. Three clones were found to bind DSG3 in Ca^{2+}-independent manner. Clone 18-1 that had the highest binding- affinity to mouse DSG3 was selected as the final candidate.

4. Screening with keratinocyte sheets is used to judge the ability of interference to adhesive function by antibodies, as the antibody which could induce PV-like lesion has dissociating activity to cell-cell adhesion. We tested clone 18-1 on the keratinocyte sheets and found there was no dissociating activity.

By this screening system an antibody with no severe side effects, 18-1, was obtained. Next, anti-tumor activity was evaluated in mice subcutaneously inoculated with a mouse lung cancer cell line LC12 overexpressing DSG3. Consequently PV-like changes were not observed in mice and the tumor was regressed by anti-mouse DSG3 antibody administration. The results show that it is possible to generate a therapeutic antibody against DSG3 by selecting an ADCC-promoting epitope that can be distinguished from an epitope inducing pathogenic response.

Next, along with the same screening flow used in generating the anti-mouse DSG3 antibody, an anti-human DSG3 antibody with high ADCC activity DF366 that does not induce PV-like lesions, was successfully generated. The potential of the DF366 antibody as a therapeutic was shown by the efficacy in xenograft models of various human squamous cell carcinomas.

III. Summary

The essential points for generating antibodies with an intended epitope are 1) the utilization of protein with functional and native conformation for *in vivo* immunization and screening, and 2) to confirm adequate function by epitope classification. These steps present a useful approach to identify and generate an antibody with intended function.

Currently, promising target molecules for antibody therapeutics are said to be exhausted. It was suggested in the second report that there is a potential for developing a novel therapeutic antibody in the choice of epitope, even if the antigen has a concern of unwanted effects as a therapeutic target. The current study may expand the option for selecting antibody-based drug targets, and is thought to contribute to the research and development for the future antibody therapeutics.

A part of this thesis was published below.

1. **Generation and characterization of monoclonal antibodies against human LGR6.**
   Funahashi SI, Suzuki Y, Nakano K, Kawai S, Suzuki M.
   "This is a pre-copyedited, author-produced version of an article accepted for publication in The Journal of Biochemistry following peer review. The version of record [The Journal of Biochemistry (2017) 161(4): 361-368] is available online at: https://doi.org/10.1093/jb/mvw077"

2. **Generation of an anti-desmoglein 3 antibody without pathogenic activity of pemphigus vulgaris for therapeutic application to squamous cell carcinoma**
   Funahashi SI, Kawai S, Fujii E, Taniguchi K, Nakano K, Ishikawa S, Aburatani H, Suzuki M.
   The Journal of Biochemistry (2018) 164(6): 471-481.
   https://doi.org/10.1093/jb/mvy074

謝辞

本研究の論文作成にあたり、終始ご指導を頂き、ご高閲を賜った麻布大学・島田章則教授に甚大なる感謝の意を表します。また本研究の遂行と論文作成にあたり種々のご指導・ご鞭撻を頂きました株式会社未来創薬研究所・鈴木雅実博士、上参郷慶一博士、藤井悦子博士に感謝の意を表します。

加えて、本研究を遂行するにあたり幹細胞研究でのモノクローナル抗体の重要性の気づきを与えていただき、温かい励ましと継続的なご支援を賜りました中外製薬株式会社・山崎達美博士に感謝の意を表します。

また、本研究を進めるにあたり、種々の研究のご支援を頂きました株式会社未来創薬研究所ならびに中外製薬株式会社の皆様に深く感謝いたします。

最後に日々私を励ましてくれた私の家族である妻の舟橋美香と息子の舟橋一真にも感謝いたします。

OXFORD UNIVERSITY PRESS | The Journal of Biochemistry

Draft Manuscript For Review

Generation and characterization of monoclonal antobodies against human LGR6

Journal:	*The Journal of Biochemistry*
Manuscript ID	Draft
Manuscript Type:	Regular Paper
Date Submitted by the Author:	n/a
Complete List of Authors:	Funahashi, Shin-ichi; Forerunner Pharma Research Co., Ltd., Department for Research Suzuki, Yasunori; Forerunner Pharma Research Co., Ltd., Department for Research Nakano, Kiyotaka; Forerunner Pharma Research Co., Ltd., Department for Research Kawai, Shigeto; Forerunner Pharma Research Co., Ltd., Department for Research Suzuki, Masami; Forerunner Pharma Research Co., Ltd., Department for Research
Keywords:	flow cytometry, LGR6, monoclonal antibody, R-spondin, stem cell marker
Topics:	16 Immunochemistry < BIOCHEMISTRY, 43 Tumor and Immunology < CELL

Regular Paper

Generation and characterization of monoclonal antibodies against human LGR6

Shin-ichi Funahashi, Yasunori Suzuki, Kiyotaka Nakano, Shigeto Kawai, and Masami Suzuki

Forerunner Pharma Research Co., Ltd., Komaba Open Laboratory, The University of Tokyo, 4-6-1 Komaba, Meguro-ku, Tokyo 153-8904, Japan

Running title: Generation and characterization of anti-LGR6 antibodies

Corresponding author:

Shin-ichi Funahashi,

Forerunner Pharma Research Co., Ltd., Komaba Open Laboratory,

The University of Tokyo,

4-6-1 Komaba, Meguro-ku, Tokyo 153-8904, Japan

Tel: +81-3-5452-5730, Fax: +81-3-5452-5738, e-mail: funahashi@forerunner-pharma.co.jp

Abbreviations:

7TM, seven-pass transmembrane; ECD, extracellular domain; FACS, fluorescence activated cell sorting; GPCR, G protein-coupled receptor; IHC, immunohistochemistry; LGR, leucine-rich repeat-containing GPCR; LRR, leucine-rich repeat; RSPO1, R-spondin 1

Leucine-rich repeat-containing G protein-coupled receptor 6 (LGR6) is a seven-pass transmembrane protein known to be a marker of stem cells in several organs. To understand the cell biology of LGR6-positive cells, including stem cells, we generated monoclonal antibodies (mAbs) against human LGR6. DNA immunization followed by whole-cell immunization with LGR6-expressing transfectants was performed to obtain mAbs that recognized the native form of LGR6. Hybridomas were screened by flow cytometry using LGR6-transfected cells. Because the molecules of LGR4, LGR5, and LGR6 are 50% homologous at the amino acid level, specificity of the mAbs was confirmed by transfectants expressing LGR4, LGR5, or LGR6. Three LGR6-specific mAbs were generated. Two of the three mAbs (designated 43A6 and 43D10) recognized the large N-terminal extracellular domain of LGR6, and competitively blocked the binding of R-spondin 1, which is known to be the ligand for LGR6. The other mAb, 43A25, recognized the seven-pass transmembrane domain of LGR6, and was able to be used for immunoblot analysis. In addition, mAbs 43A6 and 43D10 detected endogenous expression of LGR6 in cancer cell lines. We expect that our mAbs will contribute to further understanding of LGR6-positive cells in humans.

Keywords: flow cytometry/LGR6/monoclonal antibody/R-spondin/stem cell marker

Leucine-rich repeat-containing G protein-coupled receptor 6 (LGR6) is a member of the type-B LGR subfamily consisting of LGR4, LGR5, and LGR6 (*1, 2*). A structural feature of this subfamily is a large N-terminal extracellular domain (ECD) composed of 17 leucine-rich repeats (LRRs). LGR6 shares nearly 50% identity with LGR4 and LGR5 at the amino acid level (*3*). These molecules bind to R-spondins (RSPOs) through the N-terminal ECD and regulate Wnt signaling (*4-8*).

LGR6 is reported to be a stem cell marker in some organs. By mouse lineage tracing experiments, it was discovered that LGR6 is expressed in a tight cell cluster at the isthmus of the hair follicle in skin and that cells in this cluster could generate all skin components, including hair follicles, sebaceous glands, and interfollicular epidermis, in adult mice (*9, 10*). Recently, it has also been shown in mice and humans that LGR6-positive cells have stem cell properties in lungs, teeth, cochlea, and taste buds (*11-17*). To extend this knowledge from mouse experiments to humans, well-validated specific antibodies against LGR6 are mandatory. However, it is generally considered that generation of antibodies against GPCRs including those of the LGR family is difficult because of their low levels of expression and complex conformation (*18, 19*).

Previously, we compared various immunization methods to obtain monoclonal antibodies (mAbs) against LGR5 (*20*), which is known to be a marker of intestinal stem cells and colon cancer stem cells (*21, 22*). By combining DNA immunization and whole-cell immunization, we successfully generated antibodies suitable for use in flow cytometry . By using these antibodies, we could sort LGR5-positive cells from colon cancer tissues and could characterize their cancer stem cell features such as high-tumor initiating activity (*20*).

In the current study we attempted to generate human LGR6 antibodies by adapting the methods we had previously successfully used for LGR5 antibodies (*20*). As a result, we obtained LGR6-specific antibodies suitable for use in flow cytometry and for immunoblotting. Since to the best our knowledge there are no other specific antibodies against LGR6, it is expected that our antibodies will contribute to further understanding of biological insights into LGR6-positive cells in humans.

Materials and Methods

DNA constructs

LGR6 cDNA (RefSeq: NM_001017403) was PCR-amplified from Kuramochi cells. Human *LGR4* (RefSeq: NM_018490), *LGR5* (RefSeq: NM_003667), and *LGR6* genes were cloned in pCOS2 vector and expressed under EF1α promoter (*23*). For LGR4, 24 amino acids of the signal sequence of LGR4 were replaced with the signal sequence of bovine prolactin and an HA-tag was attached to the N-terminal. For analysis of the binding regions of LGR6 antibodies, full-length LGR6 and LGR6 Δ1–444 (deleted aa 1–444) were cloned in oriP/EBNA-1 episomal vector. Human *RSPO1* cDNA (RefSeq: NM_001242908) was PCR-amplified from HCC1419 cells and cloned into episomal vector with a myc-His tag in the C-terminal.

Cell culture and transfection

Mouse pro-B cell line Ba/F3 was purchased from Riken Cell Bank (Tsukuba, Japan) and cultured in RPMI-1640 medium containing 10% fetal calf serum in the presence of 1 ng/mL IL-3. Ba/F3 cell lines expressing HA-LGR4, LGR5, and LGR6 were established by electroporation with the plasmids carrying each of the LGR genes. These cell lines were selected by 500 μg/mL geneticin (Life Technologies, Tokyo, Japan). The full-length LGR6 and deletion mutant plasmid were transfected in FreeStyle 293F cells by using FreeStyle Max reagent (Life Technologies). Cells were cultured for 2 days in FreeStyle Expression Medium (Life Technologies) after transfection and were analyzed by flow cytometry. Mouse myeloma cell line P3-X63Ag8U1 was obtained from ATCC (Manassas, VA) and the cells were used as partner cells in hybridoma generation. Cancer cell lines AsPC-1, SW620, LoVo, Capan-1, PANC-1, HT-29, AGS, and HCC1419 were obtained from ATCC. Kuramochi cells were obtained from JCRB (Tokyo, Japan) and HCT 116 cells were obtained from ECACC (Salisbury, UK). Cell culture was done according to the vendors' instructions.

Animals

6-week-old Balb/c mice were purchased from Nihon Charles River (Kanagawa, Japan). Care and use of animals used in this study was in accordance with the Guidelines for the Care and Use of Laboratory Animals at Forerunner Pharma Research Co., Ltd. under the approval of the company's Institutional Animal Care and Use Committee.

Generation of antibodies

To obtain monoclonal antibodies (mAbs) against LGR6, DNA immunization (*24*) and whole-cell immunization was performed. DNA immunization was performed by the Helios Gene Gun System (Bio-Rad, Hercules, CA), with plasmid LGR6/pCOS2 coated onto 1-μ gold particles (Bio-Rad); the plasmid-coated gold particles were introduced into the abdominal epidermis of 6-week-old Balb/c mice. After eight gene-gun deliveries, when the serum titer of anti-LGR6 antibodies had increased, the mice were administered booster immunization with 2×10^6 cells of LGR6_Ba/F3. Splenocytes were isolated and fused with P3-X63Ag8U1 by the polyethylene glycol method (*25*). The resulting hybridomas were selected by culturing in hypoxanthine/aminopterin/thymidine (HAT) medium. The supernatant was screened by flow cytometry with LGR6_Ba/F3. Positive hybridomas were cloned by the limited dilution method. The mAbs were purified by HiTrap Protein G column (GE Healthcare, Tokyo, Japan). Isotyping was done with IsoStrip Mouse Monoclonal Antibody Isotyping Kit (Roche Diagnostics, Tokyo, Japan).

Flow cytometry analysis

Cells were harvested and washed with FACS buffer (2% BSA/PBS/0.05% NaN_3), and incubated with mAb at 4°C for 30 min. Then, the cells were washed with FACS buffer and stained with goat $F(ab')_2$ fragment anti- ouse IgG (Fc gamma) labeled with FITC, PE, or APC (BD Bioscience, San Jose, CA) at 4°C for 1 h. Prior to analysis, dead cells were labeled with viability dye 7-AAD (Beckman Coulter, Tokyo, Japan) or DAPI (4′,6-diamidino-2-phenylindole). Flow cytometry was performed using FACSCalibur (BD Bioscience) or FACSAria III (BD Bioscience). Flow cytometry data were analyzed using CellQuest software (BD Bioscience) and FlowJo (Tree Star, Ashland, OR).

The geometric values (geomean) values of flow cytometry analysis were plotted against the concentrations of antibodies. Graphs were drawn and EC_{50} values were estimated with GraphPad Prism (GraphPad Software, San Diego, CA). Anti-LGR5 antibody 2L36 was generated in our previous study (*20*). HA-tag antibody (HA-7) was purchased from Sigma-Aldrich (St. Louis, MO).

Immunoblot analysis

Whole-cell lysate was prepared with lysis buffer (0.5% NP-40/20 mM Tris-HCl [pH 8]/150 mM NaCl) with Complete Mini Protease Inhibitor (Roche Diagnostics). A 1 μg quantity of lysate was separated by a 4%–20% gradient SDS-PAGE and transferred to PVDF membrane (Millipore, Tokyo, Japan). Blotted protein was detected with mouse mAbs and anti- ouse IgG horseradish peroxidase conjugate (GE Healthcare). Signals were detected using the ECL Prime Western Blotting Detection System (GE Healthcare) with imaging on an ImageQuant LAS-4000 system (Fujifilm, Tokyo, Japan). For immunoblot detection of LGR5, anti-LGR5 antibody 2U1E-1 was used. The antibody 2U1E-1 was established in our previous work (*20*).

Real-time PCR

Total RNA was isolated with an RNeasy Mini Kit (Qiagen, Tokyo, Japan). Real-time PCR (qPCR) analysis of *LGR6* mRNA was performed using a StepOnePlus Real-Time PCR System (Applied Biosystems, Foster City, CA) with the following primers: LGR6F: 5′-ggcgggacagaacctctc-3′ and LGR6R: 5′-tgaggttgttcatgctgaggt-3′. Relative expression values were calculated using the $2^{-\Delta\Delta C_T}$ ethod (*26*). Beta-actin was used as a reference.

Small interfering RNA (siRNA)

LGR6 Stealth siRNA (HSS127002) was purchased from Life Technologies and introduced into AsPC-1 cells by reverse liposome transfection (lipofection) using Lipofectamine RNAiMAX transfection reagent (Life Technologies). Briefly, 30 pmol siRNA was mixed with RNAiMAX reagent and Opti-MEM medium (Life Technologies) directly in 6-well plates, and 2.5×10^5 AsPC-1

cells were then added. The transfection mix was then incubated for 48 h at 37°C in a CO_2 incubator. Cells were collected for RNA preparation and flow cytometry analysis.

Epitope analysis by competition assay

Antibodies 43A6, 43A25, and 43D10 were labeled (Alexa-488–labeled) with Alexa Fluor 488 Monoclonal Antibody Labeling Kit (Life Technologies). Competition assay was done as follows: 2×10^5 cells of LGR6_Ba/F3 were first incubated with an unlabeled antibody at 30 µg/mL for 60 min at 4°C and then incubated similarly with an Alexa-488–labeled antibody at 1 µg/mL. The cells were analyzed by flow cytometry as described above.

Competition assay for RSPO1 binding

Recombinant RSPO1- yc-His was expressed in FreeStyle 293F cells in FreeStyle 293 Expression Medium (Life Technologies) and purified with HisTrap FF column (GE Healthcare). In the RSPO1 binding assay, Ba/F3 transfectants and parental Ba/F3 cells were incubated with RSPO1- yc-His on ice for 2 h, then with anti- yc PE conjugate (9E10) (R&D Systems, Minneapolis, MN) on ice for 1 h. The cells were analyzed by flow cytometry. In the competition assay, LGR6_Ba/F3 and LGR5_Ba/F3 were pre-incubated with anti-LGR6 or anti-LGR5 antibody; they were then incubated with RSPO1- yc-His and analyzed by flow cytometry.

Results

Generation and flow cytometric analysis of anti-LGR6 mAbs

To generate anti-LGR6 mAbs suitable for use in flow cytometry, we adopted a strategy of DNA immunization followed by whole-cell immunization together with screening of hybridomas with flow cytometry.

We first established stable cell lines expressing LGR6 to use in whole-cell immunization and screening. We attempted to express LGR6 in commonly used host cells, but we failed to obtain high levels of LGR6 expression with CHO and HEK293 cells. Therefore, we transfected LGR6 cDNA into the mouse pro-B cell line Ba/F3. LGR6 was efficiently expressed on the cell surface of the transfected Ba/F3 cells. To analyze the selectivity of the hybridomas, we also prepared LGR4- and LGR5-expressing transfectants using Ba/F3 cells. LGR5 expression was confirmed by LGR5-specific antibody 2L36 as we reported previously (*20*). Because mouse LGR4 is expressed endogenously in Ba/F3 cells, HA-tagged human LGR4 was introduced and its expression was confirmed by anti-HA-tag mAbs.

Next we performed DNA immunization of Balb/c mice by using a gene gun system, followed by whole-cell immunization with LGR6-expressing transfectants. Nineteen hybridomas were selected by flow cytometry screening. We further analyzed the binding selectivity of the antibodies with LGR4- or LGR5-expressing Ba/F3 cells. Monoclonal antibodies selected were 43A6, 43A25, and 43D10, which bound to LGR6-expressing Ba/F3 but not to parent Ba/F3 or to LGR4- or LGR5-expressing transfectants (Fig. 1A).

The isotypes of LGR6-specific mAbs 43A6, 43A25 and 43D10 were IgG1/κ, IgG2a/κ and IgG1/κ, respectively. These mAbs bound to LGR6 transfectants in a dose-dependent manner, and the EC_{50} values were 664.8 ±174.5, 1438.3 ±392.0 and 630.9±185.8 ng/mL, respectively, for 43A6, 43A25 and 43D10 (mean ± SD) (Fig. 1B).

Detection of LGR6 endogenously expressed on the cell surface of various cell lines

Generally, the expression levels of most GPCR proteins including those of the LGR family are not so high. Therefore, we investigated whether the anti-LGR6 mAbs could detect endogenous LGR6 expressed in various cell lines. LGR6-expressing cell lines were searched for in the expression profile database of the Cancer Cell line Encyclopedia (CCLE) (http://www.broadinstitute.org/ccle), and pancreatic cancer cell line AsPC-1 and colorectal cancer cell line SW620 were selected. Then we analyzed the *LGR6* expression in nine cell lines, including AsPC-1 and SW620, by qPCR. AsPC-1 and SW620 showed comparatively high expression of *LGR6* at the mRNA level (Fig. 2A). When the anti-LGR6 mAbs were applied to these two cell lines, 43A6 and 43D10 were shown to bind to AsPC-1, but binding was not detected with 43A25 (Fig. 2B). The binding of 43A6 and 43D10 with respect to SW620 was minimal, reflecting the lower expression of *LGR6* mRNA in SW620.

Next we performed a knockdown experiment by *LGR6* siRNA to confirm whether the binding of 43A6 and 43D10 to AsPC-1 was dependent upon the specific binding to LGR6. At 2 days after lipofection with siRNA, expression of *LGR6* mRNA was assessed by qPCR. A significant decrease (78% decrease) in *LGR6* was observed at the mRNA level (data not shown). After introducing the siRNA into AsPC-1 cells, the binding of 43A6 and 43D10 was not detected (Fig. 2C). These results indicated that 43A6 and 43D10 could detect endogenously expressed LGR6 specifically.

Immunoblot analysis with anti-LGR6 mAbs

In addition, we also screened for mAbs able to be used for immunoblot analysis. Using the cell lysate of LGR6-expressing Ba/F3 transfectants, 43A25 clearly detected a band of approximately 100 kDa and a band exceeding 200 kDa (Fig. 3), whereas the other antibodies did not (data not shown). The molecular weight of LGR6 matched the 100 kDa band detected by 43A25, which corresponds to a monomer of LGR6, and the other ≥200 kDa band might be a dimer of LGR6. Expression of LGR4 and LGR5 in Ba/F3 transfectants was confirmed with anti-HA-tag mAb and anti-LGR5 mAb 2U1E-1, respectively (Fig. 3). Because 43A25 did not detect corresponding bands

in the blots of the LGR4 and LGR5 transfectants or the parent Ba/F3 cells, it confirms that this clone detects LGR6 specifically with immunoblotting. The 43A25 could not detect the low levels of endogenous expression of LGR6 in the whole-cell lysate of AsPC-1 (data not shown).

Characterization of the binding regions of anti-LGR6 mAbs

We classified the mAbs that were suitable for use in flow cytometry by their binding regions on LGR6. Because members of the LGR family have large N-terminal ECDs and seven-pass transmembrane (7TM) domains, we constructed an ECD deletion mutant of LGR6 (LGR6 Δ1–444). Transient expression of the deletion mutant in 293F cells was used for this analysis, because stable transfection of the deletion mutant was not obtained in Ba/F3 cells. As shown in Figure 4A, 43A25 bound to both Δ1–444 deletion mutant LGR6 and full-length LGR6, but 43A6 and 43D10 only bound to full-length LGR6. These results suggest that 43A25 recognized extracellular loops in the 7TM domain, and 43A6 and 43D10 recognized the N-terminal ECD.

We further analyzed the vicinity of epitopes of 43A6 and 43D10, both of which recognize the N-terminal domain of LGR6. Competition flow cytometry was carried out by analyzing whether mAbs labeled with Alexa-488 could bind to LGR6_Ba/F3 pre-incubated with an excess amount of another unlabeled antibody. Alexa-488–labeled 43A6 bound to LGR6_Ba/F3 pre-treated with unlabeled 43D10 (Fig. 4B, center of top panel). Alexa-488–labeled 43D10 also bound to LGR6_Ba/F3 pre-treated with unlabeled 43A6 (Fig. 4B, left of middle panel). When the Alexa-488–labeled mAbs were applied to the cells pre-incubated with the same unlabeled antibody, the binding was blocked. These results indicate that the epitopes of clones 43A6 and 43D10 are not identical in the N-terminal ECD. In addition, 43A25, which recognized the 7TM domain of LGR6, did not compete for binding with mAbs recognizing the N-terminal ECD.

Comparison of binding sites of RSPO1 and anti-LGR6 antibodies on LGR6

The N-terminal ECD of the LGR family is reported to be a binding region with respect to its ligands, RSPOs. Therefore, we analyzed whether anti-LGR6 mAbs inhibited the binding of RSPO1. Recombinant human RSPO1 with a C-terminal myc-His tag (RSPO1- yc-His) was prepared, and

the binding of RSPO1-myc-His to LGR6 and to LGR5 was analyzed by using Ba/F3 transfectants. RSPO1-myc-His bound to LGR6_Ba/F3 and LGR5_Ba/F3 in a dose-dependent manner, but did not bind to parent Ba/F3 cells (Fig. 5A). For validation of the assay system, we employed anti-LGR5 mAb 2L36 because its epitope is close to the binding site of RSPO1 (*20*). As expected, 2L36 dose-dependently blocked RSPO1 binding (Fig. 5B). Then we analyzed whether the binding of RSPO1 to LGR6 was blocked by anti-LGR6 antibodies. Monoclonal antibodies 43A6 and 43D10, which recognize the N-terminal ECD, competed with RSPO1-binding in an antibody dose-dependent manner (Fig. 5C). On the other hand, 43A25, which recognizes the 7TM domain of LGR6, did not inhibit RSPO1-binding.

Discussion

It is commonly thought to be difficult to generate antibodies against multi-pass membrane proteins that are expressed at low levels, such as GPCRs, including those of the LGR family (*18, 19*). We have sought to generate mAbs against the LGR family that are suitable for use in flow cytometry, and successfully obtained anti-LGR5 mAbs in a previous study (*20*) and anti-LGR6 mAbs in this study. For immunization, we performed DNA immunization followed by whole-cell immunization in order to obtain antibodies that recognized the native conformational epitope of LGR6 which contains complicated LRR and 7TM structures. For screening of hybridomas, ELISA using recombinant proteins or peptides is generally preferred for its high throughput and sensitivity. However, in our experience, ELISA screening is not suitable for obtaining antibodies against native forms of target molecules. Therefore, we chose to use flow cytometry screening using LGR6-expressing transfectants. As a result, we successfully obtained antibodies recognizing the native form of LRR and 7TM regions of LGR6.

An important issue with respect to this immunization and screening method was the establishment of transfectants that express sufficient amounts of antigen. To obtain such transfectants, we introduced LGR6 cDNA into several cell lines, and found that transfectants highly expressing LGR6 could be generated with Ba/F3 cells but not with CHO or HEK293 cells. The reason is currently unclear; however, it has been reported that Ba/F3 cells have been utilized as a host adequate for heterologous expression of functional GPCR (*27-29*) and are superior to CHO cells in some cases (*27*).

The antibodies we obtained in the current study are expected to be utilized in various experiments to understand the biology of LGR6-positive cells in humans. Since LGR6 is expected to be expressed in stem cells, LGR6-positive cells might be rare in organs. By using the LGR6 antibodies applicable to flow cytometry, it would be possible to analyze percentages of LGR6-positive cells, as well as their biological nature and gene expression profiles, by cell sorting. In addition, as shown in Figure 5C, mAbs 43A6 and 43D10 competitively blocked the binding of RSPO1 to LGR6. Although it is not yet confirmed whether these mAbs inhibit the RSPO signal

transmission in cells, the antibodies might be useful for understanding LGR6-dependent signaling in stem cells and cancer cells. Immunohistochemical analysis would also useful to understand the localization of LGR6-expressing cells in organs and tissues, but unfortunately, we could not obtain antibodies suitable for use in immunohistochemical analysis. Generation of such antibodies is expected in further studies.

The results of the competition analyses suggest the region of LGR6 that binds to RSPO1. In the case of LGR4 and LGR5, crystal structure analysis has shown that RSPO1 recognizes LRR3 to LRR9 of the N-terminal ECD (*30*-*33*). But the binding region of LGR6 has not yet been reported. Here, anti-LGR6 antibodies 43A6 and 43D10 recognized the N-terminal ECD of LGR6 and blocked RSPO1 binding to LGR6. These findings suggest that RSPO1 binds to LGR6 via its N-terminal LRR domain, similarly to LGR4 and LGR5.

In the skin, LGR6-positive cells differentiate to all kinds of skin cells which constitute the epidermis, such as skin, hair follicles, sebaceous glands, and interfollicular dermis (*9*). With respect to regenerative medicine in dermatology, the application of LGR6-positive stem cells is considered for the treatment of skin injuries (*34*-*38*). In this study, we generated anti-human LGR6 antibodies able to be used in flow cytometry and for immunoblot analysis. We expect that these antibodies will contribute to expanding our knowledge of the biology of LGR6-positive cells in regenerative medicine as well as in oncology.

Acknowledgements

We express our thanks to Ms. Kaori Matsumoto, Ms. Aiko Kawashima, Ms. Kumiko Nakajima, Ms. Akiko Hasebe, and Mr. Masaya Yamazaki for their skillful assistance. And, for his continuous encouragement and support for research at Forerunner Pharma Research, we also thank Dr. Tatsumi Yamazaki, who realized the importance of monoclonal antibodies against members of the LGR family for stem cell biology research.

Conflict of Interest

The authors are employees of Forerunner Pharma Research Co., Ltd. founded by Chugai Pharmaceutical Co., Ltd., and declare no other potential conflict of interest.

REFERENCES

1. Luo, C.W. and Hsueh, A.J. (2006) Genomic analyses of the evolution of LGR genes. *Chang Gung Med. J.* **29**, 2–8
2. Van Hiel, M.B., Vandersmissen, H.P., Van Loy, T., and Vanden Broeck, J. (2012) An evolutionary comparison of leucine-rich repeat containing G protein-coupled receptors reveals a novel LGR subtype. *Peptides* **34**, 193–200
3. Hsu, S.Y., Kudo, M., Chen, T., Nakabayashi, K., Bhalla, A., van der Spek, P.J., van Duin, M., and Hsueh, A.J. (2000) The three subfamilies of leucine-rich repeat-containing G protein-coupled receptors (LGR): identification of LGR6 and LGR7 and the signaling mechanism for LGR7. *Mol. Endocrinol.* **14**, 1257–1271
4. Carmon, K.S., Gong, X., Lin, Q., Thomas, A., and Liu, Q. (2011) R-spondins function as ligands of the orphan receptors LGR4 and LGR5 to regulate Wnt/β-catenin signaling. *Proc. Natl. Acad. Sci. USA* **108**, 11452–11457
5. de Lau, W., Barker, N., Low, T.Y., Koo, B.K., Li, V.S., Teunissen, H., Kujala, P., Haegebarth, A., Peters, P.J., van de Wetering, M., Stange, D.E., van Es, J.E., Guardavaccaro, D., Schasfoort, R.B., Mohri, Y., Nishimori, K., Mohammed, S., Heck, A.J., and Clevers, H. (2011) Lgr5 homologues associate with Wnt receptors and mediate R-spondin signalling. *Nature* **476**, 293–297
6. Ruffner, H., Sprunger, J., Charlat, O., Leighton-Davies, J., Grosshans, B., Salathe, A., Zietzling, S., Beck, V., Therier, M., Isken, A., Xie, Y., Zhang, Y., Hao, H., Shi, X., Liu, D., Song, Q., Clay, I., Hintzen, G., Tchorz, J., Bouchez, L.C., Michaud, G., Finan, P., Myer, V.E., Bouwmeester, T., Porter, J., Hild, M., Bassilana, F., Parker, C.N., and Cong, F. (2012) R-Spondin potentiates Wnt/β-catenin signaling through orphan receptors LGR4 and LGR5. *PloS One* **7**, e40976
7. Glinka, A., Dolde, C., Kirsch, N., Huang, Y.L., Kazanskaya, O., Ingelfinger, D., Boutros, M., Cruciat, C.M., and Niehrs, C. (2011) LGR4 and LGR5 are R-spondin receptors mediating Wnt/β-catenin and Wnt/PCP signalling. *EMBO Rep.* **12**, 1055–1061

8. Gong, X., Carmon, K.S., Lin, Q., Thomas, A., Yi, J., and Liu, Q. (2012) LGR6 is a high affinity receptor of R-spondins and potentially functions as a tumor suppressor. *PloS One* **7**, e37137
9. Snippert, H.J., Haegebarth, A., Kasper, M., Jaks, V., van Es, J.H., Barker, N., van de Wetering, M., van den Born, M., Begthel, H., Vries, R.G., Stange, D.E., Toftgård, R., and Clevers, H. (2010) Lgr6 marks stem cells in the hair follicle that generate all cell lineages of the skin. *Science* **327**, 1385–1389
10. Snippert, H.J. and Clevers, H. (2011) Tracking adult stem cells. *EMBO Rep*. **12**, 113–122
11. Oeztuerk-Winder, F., Guinot, A., Ochalek, A., and Ventura, J.J. (2012) Regulation of human lung alveolar multipotent cells by a novel p38α MAPK/miR-17-92 axis. *EMBO J*. **31**, 3431–3441
12. Ruiz, E.J., Oeztuerk-Winder, F., and Ventura, J.J. (2014) A paracrine network regulates the cross-talk between human lung stem cells and the stroma. *Nat. Commun*. **5**, 3175
13. Kitamura, J., Uemura, M., Kurozumi, M., Sonobe, M., Manabe, T., Hiai, H., Date, H., and Kinoshita, K. (2015) Chronic lung injury by constitutive expression of activation-induced cytidine deaminase leads to focal mucous cell metaplasia and cancer. *PloS One* **10**, e0117986
14. Kawasaki, M., Porntaveetus, T., Kawasaki, K., Oommen, S., Otsuka-Tanaka, Y., Hishinuma, M., Nomoto, T., Maeda, T., Takubo, K., Suda, T., Sharpe, P.T., and Ohazama, A. (2014) R-spondins/Lgrs expression in tooth development. *Dev. Dyn.* **243**, 844–851
15. Zhang, Y., Chen, Y., Ni, W., Guo, L., Lu, X., Liu, L., Li, W., Sun, S., Wang, L., and Li, H. (2015) Dynamic expression of Lgr6 in the developing and mature mouse cochlea. *Front. Cell. Neurosci*. **9**, 165
16. Yee, K.K., Li, Y., Redding, K.M., Iwatsuki, K., Margolskee, R.F., and Jiang, P. (2013) Lgr5-EGFP marks taste bud stem/progenitor cells in posterior tongue. *Stem Cells* **31**, 992–1000
17. Ren, W., Lewandowski, B.C., Watson, J., Aihara, E., Iwatsuki, K., Bachmanov, A.A., Margolskee, R.F., and Jiang, P. (2014) Single Lgr5- or Lgr6-expressing taste stem/progenitor cells generate taste bud cells ex vivo. *Proc. Natl. Acad. Sci. USA* **111**, 16401–16406

18. Jo, M. and Jung, S.T. (2016) Engineering therapeutic antibodies targeting G-protein-coupled receptors. *Exp. Mol. Med*. **48**, e207

19. Hutchings, C.J., Koglin, M., and Marshall, F.H. (2010) Therapeutic antibodies directed at G protein-coupled receptors. *MAbs* **2**, 594–606

20. Kobayashi, S., Yamada-Okabe, H., Suzuki, M., Natori, O., Kato, A., Matsubara, K., Jau Chen, Y., Yamazaki, M., Funahashi, S., Yoshida, K., Hashimoto, E., Watanabe, Y., Mutoh, H., Ashihara, M., Kato, C., Watanabe, T., Yoshikubo, T., Tamaoki, N., Ochiya, T., Kuroda, M., Levine, A.J., and Yamazaki, T. (2012) LGR5-positive colon cancer stem cells interconvert with drug-resistant LGR5-negative cells and are capable of tumor reconstitution. *Stem Cells* **30**, 2631–2644

21. Barker, N., van Es, J.H., Kuipers, J., Kujala, P., van den Born, M., Cozijnsen, M., Haegebarth, A., Korving, J., Begthel, H., Peters, P.J., and Clevers, H. (2007) Identification of stem cells in small intestine and colon by marker gene Lgr5. *Nature* **449**, 1003–1007

22. Leushacke, M. and Barker, N. (2012) Lgr5 and Lgr6 as markers to study adult stem cell roles in self-renewal and cancer. *Oncogene* **31**, 3009–3022

23. Konishi, H., Okamoto, K., Ohmori, Y., Yoshino, H., Ohmori, H., Ashihara, M., Hirata, Y., Ohta, A., Sakamoto, H., Hada, N., Katsume, A., Kohara, M., Morikawa, K., Tsukuda, T., Shimma, N., Foster, G.R., Alazawi, W., Aoki, Y., Arisawa, M., and Sudoh, M. (2012) An orally available, small-molecule interferon inhibits viral replication. *Sci. Rep*. **2**, 259

24. Chua, K.Y., Ramos, J.D., and Cheong, N. (2008) Production of monoclonal antibody by DNA immunization with electroporation. *Methods Mol. Biol*. **423**, 509–520

25. Galfrè, G. and Milstein, C. (1981) Preparation of monoclonal antibodies: strategies and procedures. *Methods Enzymol*. **73**, 3–46

26. Livak, K.J. and Schmittgen, T.D. (2001) Analysis of relative gene expression data using real-time quantitative PCR and the $2^{-\Delta\Delta C_T}$ method. *Methods*. **25**, 402–408

27. Wang, S., Clemmons, A., Bayne, M., and Graziano, M.P. (1998) Retrovirus-mediated expression of the GalR1 galanin receptor: implication for efficient stable expression of functional G protein-coupled receptors. *J. Recept. Signal Transduct. Res*. **18**, 311–320

28. Kashima, K., Watanabe, M., Sato, Y., Hata, J., Ishii, N., and Aoki, Y. (2014) Inhibition of metastasis of rhabdomyosarcoma by a novel neutralizing antibody to CXC chemokine receptor-4. *Cancer Sci*. **105**, 1343–1350

29. Yamauchi, T., Kamon, J., Ito, Y., Tsuchida, A., Yokomizo, T., Kita, S., Sugiyama, T., Miyagishi, M., Hara, K., Tsunoda, M., Murakami, K., Ohteki, T., Uchida, S., Takekawa, S., Waki, H., Tsuno, N., Shibata, Y., Terauchi, Y., Froguel, P., Tobe, K., Koyasu, S., Taira, K., Kitamura, T., Shimizu, T., Nagai, R., and Kadowaki, T. (2003) Cloning of adiponectin receptors that mediate antidiabetic metabolic effects. *Nature* **423**, 762–769

30. Chen, P.H., Chen, X., Lin, Z., Fang, D., and He, X. (2013) The structural basis of R-spondin recognition by LGR5 and RNF43. *Genes Dev*. **27**, 1345–1350

31. Peng, W.C., de Lau, W., Forneris, F., Granneman, J.C., Huch, M., Clevers, H., and Gros, P. (2013) Structure of stem cell growth factor R-spondin 1 in complex with the ectodomain of its receptor LGR5. *Cell Rep*. **3**, 1885–1892

32. Wang, D., Huang, B., Zhang, S., Yu, X., Wu, W., and Wang, X. (2013) Structural basis for R-spondin recognition by LGR4/5/6 receptors. *Genes Dev*. **27**, 1339–1344

33. Xu, J.G., Huang, C., Yang, Z., Jin, M., Fu, P., Zhang, N., Luo, J., Li, D., Liu, M., Zhou, Y., and Zhu, Y. (2015) Crystal structure of LGR4–Rspo1 complex: insights into the divergent mechanisms of ligand recognition by leucine-rich repeat G-protein-coupled receptors (LGRs). *J. Biol. Chem*. **290**, 2455–2465

34. Blanpain, C. (2010) Stem cells: skin regeneration and repair. *Nature* **464**, 686–687

35. Lough, D., Dai, H., Yang, M., Reichensperger, J., Cox, L., Harrison, C., and Neumeister, M.W. (2013) Stimulation of the follicular bulge LGR5+ and LGR6+ stem cells with the gut-derived human alpha defensin 5 results in decreased bacterial presence, enhanced wound healing, and hair growth from tissues devoid of adnexal structures. *Plast. Reconstr. Surg*. **132**, 1159–1171

36. Lough, D.M., Wetter, N., Madsen, C., Reichensperger, J., Cosenza, N., Cox, L., Harrison, C., and Neumeister, M.W. (2016) Transplantation of an LGR6+ epithelial stem cell-enriched scaffold for repair of full-thickness soft-tissue defects: the in vitro development of polarized hair-bearing skin. *Plast. Reconstr. Surg*. **137**, 495–507

37. Lough, D.M., Yang, M., Blum, A., Reichensperger, J.D., Cosenza, N.M., Wetter, N., Cox, L.A., Harrison, C.E., and Neumeister, M.W. (2014) Transplantation of the LGR6+ epithelial stem cell into full-thickness cutaneous wounds results in enhanced healing, nascent hair follicle development, and augmentation of angiogenic analytes. *Plast. Reconstr. Surg*. **133**, 579–590

38. Solanas, G. and Benitah, S.A. (2013) Regenerating the skin: a task for the heterogeneous stem cell pool and surrounding niche. *Nat. Rev. Mol. Cell Biol*. **14**, 737–748

Figure Legends

Figure 1. Flow cytometric analysis of anti-LGR6 mAbs

(A) Binding specificity was evaluated with HA-LGR4, LGR5, and LGR6-transfected Ba/F3 by flow cytometry. Two μg/mL of anti-LGR6 mAbs (black line) or control isotype mAb (black shading) were reacted with HA-LGR4, LGR5, LGR6-transfected Ba/F3, or parent Ba/F3 (results are mean ± SD., n=3). As a control, 2L36 (for LGR5) (*20*) and HA-7 (for HA-LGR4) were used. Binding was detected by PE-conjugated anti-mouse antibody.

(B) Dose-dependent binding was evaluated with LGR6_Ba/F3 (left) and parent Ba/F3 (right). Cells were incubated with the indicated concentrations of 43A6 (closed triangles), 43A25 (closed squares), and 43D10 (open circles).

Figure 2. Detection of LGR6 endogenously expressed on the cell surface in cancer cell lines.

(A) The *LGR6* mRNA expression levels of nine cell lines were determined by real-time PCR. Relative expression level was calculated by normalizing with beta-actin.

(B) AsPC-1 and SW620 were incubated with 10 μg/mL of anti-LGR6 mAbs (black line) or control isotype mAb (black shading) and analyzed by flow cytometry.

(C) siRNA against *LGR6* (si-LGR6) or negative control (si-ctrl) were introduced to AsPC-1 cells by lipofection. After 2 days, cells were collected and binding activities of anti-LGR6 mAbs (black line) or control isotype mAb (black shading) were analyzed.

Figure 3. Immunoblot analysis of anti-LGR6 mAb

Whole-cell lysate of HA-LGR4-, LGR5-, and LGR6-transfected Ba/F3 cells and parent Ba/F3 cells was immunoblotted using 5 μg/mL of 43A25 as described in *Materials and Methods*. The expression of LGR5 and LGR4 of the transfectants was confirmed by anti-LGR5 mAb 2U1E-1 and anti-HA tag antibodies, respectively. Anti-beta actin antibody was used as control.

Figure 4. Epitope analysis of anti-LGR6 mAbs

(A) Full-length LGR6 or LGR6 Δ1–444 was expressed by 293F cells using the FreeStyle expression system as described in *Materials and Methods*. The binding activity of anti-LGR6 mAbs was analyzed by flow cytometry. Histograms show binding of anti-LGR6 mAbs (black line) or control isotype mAb (black shading).

(B) Competition assays performed by flow cytometry. LGR6-transfected Ba/F3 cells were incubated with unlabeled anti-LGR6 mAb (black line) or control IgG (gray shading) followed by Alexa-488–labeled mAb. Histograms of cells not treated with antibodies are indicated by black shading.

Figure 5. Competitive activities of mAbs on RSPO1 binding to LGR6

(A) LGR6-transfected Ba/F3 (closed squares), LGR5-transfected Ba/F3 (open circles), and parent Ba/F3 (closed triangles) were incubated with the indicated concentrations of recombinant RSPO1-myc-His. RSPO1 binding was detected by flow cytometry using anti-myc tag antibodies (results are mean ± SD, n=3).

(B) LGR5-transfected Ba/F3 cells were incubated with 2L36 (closed diamonds) or control IgG (closed circles), followed by 2 μg/mL of RSPO1-myc-His, and RSPO1 binding was analyzed by flow cytometry.

(C) LGR6-transfected Ba/F3 cells were incubated with 43A6 (closed triangles), 43D10 (open circles), 43A25 (closed squares), or control IgG (open squares) and RSPO1 binding was analyzed by flow cytometry.

Figure 1

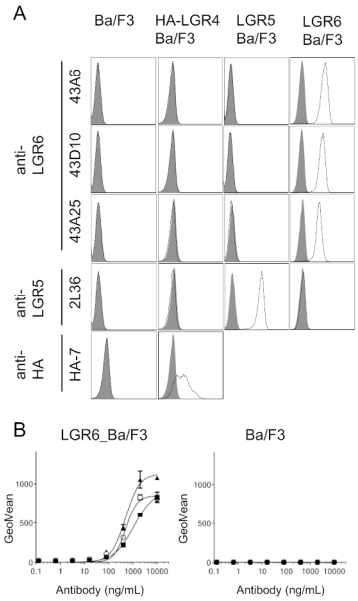

190x254mm (300 x 300 DPI)

Figure 2

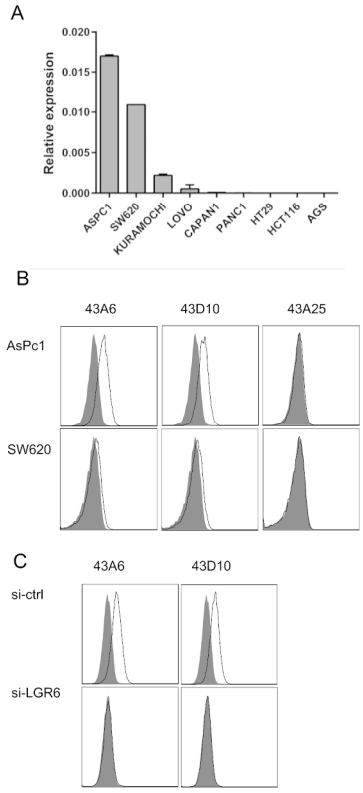

190x254mm (300 x 300 DPI)

Figure 3

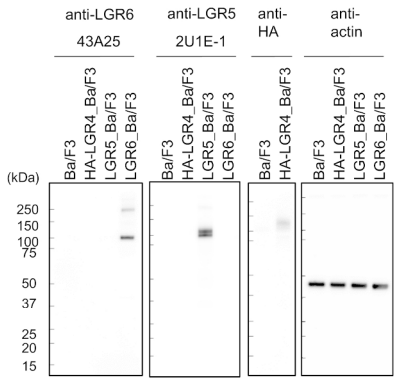

190x254mm (300 x 300 DPI)

Figure 4

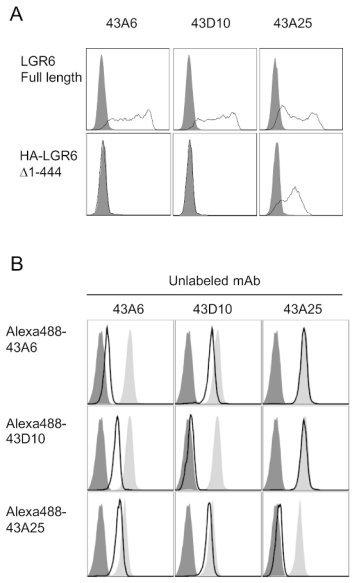

190x254mm (300 x 300 DPI)

Figure 5

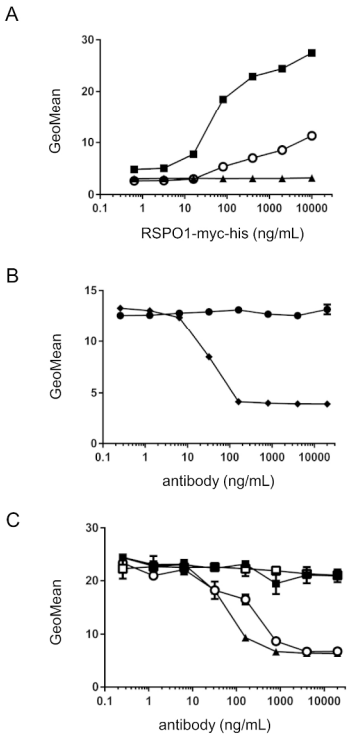

190x254mm (300 x 300 DPI)

J. Biochem. 2018;164(6):471–481 doi:10.1093/jb/mvy074

JB THE JOURNAL OF BIOCHEMISTRY

Generation of an anti-desmoglein 3 antibody without pathogenic activity of pemphigus vulgaris for therapeutic application to squamous cell carcinoma

Received January 18, 2018; accepted September 17, 2018; published online September 18, 2018

Shin-Ichi Funahashi[1,*], Shigeto Kawai[1], Etsuko Fujii[1,2], Kenji Taniguchi[2], Kiyotaka Nakano[1], Shumpei Ishikawa[3], Hiroyuki Aburatani[3] and Masami Suzuki[1,2]

[1]Forerunner Pharma Research Co., Ltd., Komaba Open Laboratory, The University of Tokyo, 4-6-1 Komaba, Meguro-ku, Tokyo 153-8904, Japan; [2]Chugai Pharmaceutical Co., Ltd., 200 Kajiwara, Kamakura, Kanagawa 247-8530, Japan and [3]Genome Science, RCAST, The University of Tokyo, 4-6-1 Komaba, Meguro-ku, Tokyo 153-8904, Japan

*Shin-Ichi Funahashi, Forerunner Pharma Research Co., Ltd., Komaba Open Laboratory, The University of Tokyo, 4-6-1 Komaba, Meguro-ku, Tokyo 153-8904, Japan.
Tel: +81-3-5452-5730, Fax: +81-3-5452-5738,
email: funahashi@forerunner-pharma.co.jp

It is ideal for the target antigen of a cytotoxic therapeutic antibody against cancer to be cancer-specific, but such antigens are rare. Thus an alternative strategy for target selection is necessary. Desmoglein 3 (DSG3) is highly expressed in lung squamous cell carcinoma, while it is well-known that anti-DSG3 antibodies cause pemphigus vulgaris, an autoimmune disease. We evaluated DSG3 as a novel target by selecting an epitope that exerts efficacy against cancer with no pathogenic effects in normal tissues. Pathogenic anti-DSG3 antibodies induce skin blisters by inhibiting the cell–cell interaction in a Ca^{2+}-dependent manner. We screened anti-DSG3 antibodies that bind DGS3 independent of Ca^{2+} and have high antibody-dependent cell cytotoxicity (ADCC) activity against DSG3-expressing cells. These selected antibodies did not inhibit cell–cell interaction and showed ADCC activity against squamous cell carcinoma cell lines. Furthermore, one of the DSG3 antibodies showed anti-tumour activity in tumour mouse models but did not induce adverse effects such as blister formation in the skin. Thus it was possible to generate an antibody against DSG3 by using an appropriate epitope that retained efficacy with no pathogenicity. This approach of epitope selection may expand the variety of druggable target molecules.

Keywords: DSG3; epitope; monoclonal antibody; pemphigus vulgaris; squamous cell carcinoma.

Abbreviations: ADCC, antibody-dependent cell cytotoxicity; DSG3, desmoglein 3; FACS, flow cytometry; mAb, monoclonal antibody; PV, pemphigus vulgaris; SCC, squamous cell carcinoma.

Therapeutic antibodies are being actively researched and used to treat an increasing number of diseases, including cancer (*1*). Therapeutic antibodies for cancer are now available with neutralizing, antibody-dependent cellular cytotoxicity (ADCC) and complement-dependent cytotoxicity (CDC) functions (*2–6*). Technologies for producing low-fucosylated or defucosylated antibodies that have enhanced ADCC have been established and applied to therapeutic antibodies (*7–9*). The ideal target molecule for a cytotoxic antibody is a cancer-specific antigen, but although research has focused on searching for such a target, almost no cancer-specific antigens have been discovered (*10*). Thus, it may be necessary to discover novel therapeutic antibodies by an alternative strategy that involves selecting an antigen with relatively high expression in cancer compared with normal tissue and designing an antibody with the appropriate anti-cancer functions against that antigen.

Desmoglein-3 (DSG3) is expressed in normal squamous epithelia and overexpressed in squamous cell carcinoma (SCC) of the lung (*11–14*). However, DSG3 is a molecule associated with pemphigus vulgaris (PV), a severe autoimmune blistering disease affecting skin and mucosa, and it is known that anti-DSG3 autoantibodies are involved in the onset of the disease (*15*, *16*). Different disease states are induced according to the different recognition sites of the anti-DSG3 antibodies. Evidence of this is that the most severe disease state is induced by antibodies that recognize the interaction sites of the EC1-EC2 domains at the N-terminal of DGS3, whereas antibodies with other recognition sites are not associated with pathogenic states (*17–19*). Because the evidence from PV suggests that there is a large difference in biological reaction according to the recognition site of an autoantibody, we hypothesized that selecting the antibody epitope carefully would make it possible to develop a novel anticancer antibody applicable for SCC that avoids the pemphigus pathogenesis.

Here we show that we have obtained an anti-mouse DSG3 monoclonal antibody (mAb) with therapeutic potential and have evaluated whether its pathogenic activity had been successfully separated from its anticancer activity. Furthermore we have attempted to generate an anti-human DSG3 mAb with the same characteristics.

Materials and Methods

Human clinical samples

The tissues evaluated in the current study are from the tissue library at PharmaLogicals Research Pte. Ltd. (PLR, Singapore) (*20*). The tissues examined in the current study included six cases of SCC (lung 2, skin 3 and uterus 1) and six cases of lung adenocarcinoma. The surgically excised tissues were provided by patients that gave their informed consent, as approved by the ethical committee at PLR in Singapore.

Animals

Dsg3 (-/-) mice (B6; 129X1-*Dsg3*^{tm1Stan}/J) were purchased from Jackson Laboratory and bred at Charles River Laboratories Japan. Severe combined immunodeficient (SCID) mice (C.B-17/lcr-*scid* Jcl) were purchased from CLEA Japan. MRL/lpr mice (MRL/MpJ-*Tnfrsf6*^{lpr}/Crlj) and Balb/c mice (BALB/cAnNCrlCrlj) were purchased from Charles River Laboratories Japan. Care and use of animals used in this study was in accordance with the Guidelines for the Care and Use of Laboratory Animals under the approval of the Institutional Animal Care and Use Committees at The University of Tokyo and Chugai Pharmaceutical Co., Ltd. Immunizations were performed in the experimental animal facility at The University of Tokyo. Mouse xenograft experiments were performed at Chugai Pharmaceutical Co., Ltd.

Cells

Chinese hamster ovary (CHO) cell line DG44, mouse B cell line Ba/F3 or human lung SCC cell lines HARA and A431 were purchased from Invitrogen, Riken Bioresource Center, and Health Science Research Resources Bank, respectively. Human NK cell lymphoma cell line NK-92, tongue SCC cell lines SCC-15 and mouse myeloma P3-X63Ag8U1 (P3U1) were obtained from the ATCC. Mouse lung SCC cell line LC-12 was purchased from NCI and maintained by subcutaneously inoculating minced tissues into Balb/c mice. Normal human keratinocyte CryoNHEK-Neo and mouse keratinocyte MPEK-BL6 were purchased from Lonza and CELLnTEC. GDP-fucose transporter (GFT) (-/-) CHO cell was obtained from Chugai Pharmaceutical Co., Ltd. (*7*). All cell cultures were conducted according to the manufacturers' instructions. Most of the reagents for cell culture were purchased from Invitrogen. Culture conditions are described in Supplementary Data.

DNA

Full-length cDNA of human DSG3 (RefSeq: NM_001944) was obtained by PCR amplification from human small intestine Marathon-Ready cDNA (Clontech). In the same manner, mouse DSG3 cDNA (RefSeq: NM_030596) was cloned from mouse E17 cDNA (Clontech). Mouse FcγRIIIa (CD16) (RefSeq: NM_010188) was cloned from mouse spleen cDNA (Clontech).

Each cDNA was cloned into the mammalian expression vector, pMCN (pMCN/human DSG3, pMCN/mouse DSG3). pMCN is vector driven under the promoter of mouse CMV and is selected with the neomycin-resistance gene.

Establishment of DSG3-expressing stable cell lines in CHO and Ba/F3 and NK92 cell lines for the ADCC assay

All transfections were carried out by electroporation with BioRad GenePulser, and stable transfectants were selected in the medium in the presence of geneticin (Invitrogen). Next, cell lines derived from single cells that had been clonally expanded were obtained by the limiting-dilution method. Electroporation was conducted under conditions of 1.5 kV, 25 μF for CHO DG44, 260 V, 1050 μF for Ba/F3 and 200 kV, 975 μF for NK92. The cells were suspended in phosphate-buffered saline (PBS) (-) at a concentration of 1×10^7 cells/ml, and were transfected with 10–25 μg of plasmid DNA. The cell surface expression of mouse or human DSG3 in the transfected cells was confirmed by flow cytometry (FACS) with AK23 antibody. CHO DG44 transduced with mouse or human DSG3 cDNA was designated as mouse DSG3/DG44 or human DSG3/DG44, respectively. The Ba/F3 transfectants were designated as mouse DSG3/BaF3 and human DSG3/BaF3.

To establish a stable assay for ADCC activity, NK92 expressing mouse FcγRIIIa (mFcγRIIIa-NK92) was established as a cell line and incorporated as effector cells. Mouse FcγRIIIa was expressed as a chimeric protein comprising the extracellular domain of mouse FcγRIIIa (aa 1-212) fused to the transmembrane domain and the cytoplasmic domain of human FcγRIIIa (aa 207-254). The cells were clonally expanded by selecting in 500 μg/ml of geneticin.

Generation of recombinant DSG3 proteins

Soluble mouse DSG3-His proteins were expressed in DG44 and affinity purified from the supernatants of the transfectants with His-Trap column (GE Healthcare).

Soluble human DSG3 was expressed as sDSG3-mIgG2aFc composed of the extracellular domain of human DSG3 (aa 1-616) and the Fc portion of mouse IgG2a, and was purified with HiTrap Protein G HP column (GE Healthcare) and eluted with 0.1 M Glycine-HCl (pH 2.7). The eluate was gel-filtrated with Superdex 200HR 10/30 (GE Healthcare).

Glutathione S-transferase (GST)-human DSG3 fusion protein (GST-hDSG3) was expressed in *Escherichia coli* as a fusion of GST and 125 aa of human DSG3 (aa 491-615) with His-tag. GST-hDSG3 was purified with His-Trap column (GE Healthcare) for use as an antigen for ELISA.

Immunohistochemical (IHC) analysis of human DSG3 in clinical samples

Human tissues were fixed in 4% paraformaldehyde upon collection, and embedded in paraffin by the AMeX method as described previously (*21*, *22*). Thin sections were prepared at a thickness of 3–5 μm for histology and IHC. IHC staining for human DSG3 in human tissues was performed using the following method. A monoclonal mouse anti-human DSG3 antibody (Clone 5G11, Zymed) was applied as the primary antibody. The tissues were stained by an indirect immunoperoxidase method using the Ventana HX Discovery System (Ventana Medical Systems). Briefly, the slides were de-waxed and treated with protein block (Dako Cytomation) to reduce non-specific staining and 3% H_2O_2 in methanol to block endogenous peroxidase. After incubation with the primary antibody and Discovery Universal Secondary Antibody (Ventana Medical Systems), streptavidin conjugated to horseradish peroxidase (Ventana Medical Systems) was applied and the reaction visualized with a diaminobenzidine solution (Ventana Medical Systems). The slides were counterstained with haematoxylin and coverslipped. The slides were read under a light microscope.

The slides were read for staining frequency (positive percentage to all tumour cells), and staining intensity (scores: 0, negative; 1, very weak; 2, weak; 3, moderate; 4, strong). The staining score was calculated by adding up the product of staining frequency to intensity scores.

Generation of anti-mouse DSG3 mAbs

mAbs against mouse DSG3 were generated by DNA immunization. A plasmid DNA expressing full length mouse *Dsg3* was inoculated into the skin of the abdomen of *Dsg3*-knockout (KO) mice using Helios Gene Gun (BioRad) followed by intravenous injection of mouse DSG3/DG44 cells as a booster immunization. At 4 days after the last immunization, splenocytes were isolated and fused with mouse myeloma P3U1 by the general polyethylene glycol method with PEG1500 (Roche Diagnostics) (*23*). The resulting hybridomas were selected by culturing in hypoxanthine/aminopterin/thymidine (HAT) medium containing RPMI-1640 medium with 10% FBS, 1-fold concentration of HAT media supplement (Sigma) and 0.5-fold concentration of BM-combined H1 Hybridoma cloning supplement (Roche Diagnostics). The culture supernatants were screened for their ability to bind to mouse DSG3 by FACS with mouse DSG3/DG44. Positive hybridomas were subcloned by the limited-dilution method. We selected 34 FACS-positive clones, measured their ADCC activity and further selected 12 candidates with strong ADCC. The 12 hybridomas, 1-2, 18-1, 33-1, 32-2, 29-2, 10-2, 20-1, 37-1, 5-1, 39-2, 19-1 and 40-2 were cultured in the medium containing HAT medium supplemented with Ultra low IgG FBS (Invitrogen), and mAbs were purified by HiTrap Protein G column (GE Healthcare). Isotyping was carried out with IsoStrip Mouse Monoclonal Antibody Isotyping Kit (Roche Diagnostics).

Generation of anti-human DSG3 mAbs

Anti-human DSG3 mAbs were generated by immunizing MRL/lpr mice and Balb/c mice of 7–8 weeks old. At the first immunization, 100 μg of soluble human DSG3 (sDSG3-mIgG2aFc) was mixed with complete Freund's adjuvant (Beckton Dickinson) and was inoculated subcutaneously. Two weeks later, 50 μg of sDSG3-mIgG2aFc was mixed with incomplete Freund's adjuvant and was inoculated subcutaneously. At 1 week intervals, booster immunization was performed two to four times, and a final immunization was carried out by injecting 50 μg of the same protein into the tail vein. At 4 days after final administration, splenocytes were isolated and fused with

P3U1 by the conventional method. The hybridoma supernatant was screened for binding activity to human DSG3 by FACS with human DSG3/DG44. Positive hybridomas were cloned by the limited-dilution method to establish monoclonal antibodies specific for human DSG3. Of the antibody clones, DF366 was selected as the mAb with the strongest ADCC activity.

FACS

Binding affinity of mAbs to the antigens was analysed as described previously (*24*, *25*). Briefly, Ba/F3 or DG44 transfectants were incubated with mAb diluted to appropriate concentrations for 1 h on ice, and then with FITC-labelled anti-mouse IgG for 30 min on ice. After reaction, the cells were analysed by FACS on a FACSCalibur flow cytometer (Beckton Dickinson).

In general, antibodies that induce PV-like states are known to show Ca^{2+}-dependent binding to mouse DSG3. Thus to select antibodies with no pathogenic activity, we screened mAbs by evaluating their Ca^{2+} independent binding activity. The mAbs were analysed as with 1 mM or without Ca^{2+} and 5 mM EDTA by FACS.

In the case of LC-12 cells, the tumour tissue was resected and disaggregated into a single cell suspension by treatment with Dispase II (Roche Diagnostics) at 37°C for 20 h.

ELISA

For GST-DSG3 ELISA, GST-hDSG3 protein was coated onto the microtiter plate at a concentration of 1 μg/ml, and blocked with 1% BSA. Then anti-human DSG3 antibodies were incubated with GST-hDSG3. The bound antibodies were detected with alkaline phosphatase (AP)-conjugated goat anti-mouse kappa antibody (Southern Biotech).

In order to classify the antibodies to subgroups by binding regions the competitive ELISA was performed as follows. After preincubation with non-labelled antibody (test antibody), biotin-labelled antibody was added, then the binding inhibition by test antibody was measured to classify the binding region. Anti-human DSG3 mAbs DF029, DF129, DF131, DF132, DF138, DF187 and DF269 were biotinylated. Biotinylation was conducted with a biotin labelling kit (Roche Diagnostics). The reaction was performed as reported before (*26*). Briefly, sDSG3-mIgG2aFc were bound onto anti-mouse IgG2a antibody-precoated microtiter plate. Then test antibodies were incubated at room temperature for 1 h, followed by incubation with biotinylated antibodies. After washing, the binding of biotinylated antibodies was detected with AP-conjugated streptavidin (Zymed). The mAbs with 90% of binding inhibition were classified as antibodies with the same binding region.

Generation of ADCC-enhanced antibody

Mouse mAbs were genetically engineered to produce antibodies of the IgG2a isotype. Total RNA was extracted from the hybridoma with the RNA easy plant mini kit (QIAGEN), and the genes encoding the mAb were amplified by reverse transcription-PCR (RT-PCR) using the method described previously (*26*). PCR products were cloned into pGEM-T Easy vector (Promega) and nucleotide sequences were determined.

A chimeric anti-DSG3 antibody, in which the mouse variable regions were linked with the mouse IgG2a and kappa constant regions or human IgG1 and kappa regions, was constructed. The light and heavy chain expression vectors were co-transfected into CHO DG44 cells and selected with geneticin. Screening clones of the well-expressed antibodies by flow cytometry with mouse DSG3/DG44 or human DSG3/DG44, we purified the chimeric antibodies with a HiTrap ProteinG column. Anti-mouse DSG3 mAb 18-1 with a mouse IgG2a isotype was designated as 18-1m, and anti-human DSG3 mAb DF366 as DF366m. Anti-human DSG3 mAb DF366 with a human IgG1 isotype was designated as DF366c.

Defucosylated antibody 18-1m or DF366m was expressed in GFT (-/-) CHO cells with disrupted GFT alleles of GFT gene (*7*) and designated as df-18-1m or df-DF366m.

Analysis of cell-cell dissociating activity

Cell–cell dissociating activity of mAbs was analysed by the keratinocyte dissociation assay described previously (*27*). Normal mouse keratinocytes (MPEK-BL6) or human keratinocytes (CryoNHEK-Neo) were used. When cells reached confluence, the culture medium was changed to the same medium containing 1.2 mM Ca^{2+}. Then antibody was added to a final concentration of 10 μg/ml. After incubation at 37°C overnight, Staphylococcal exotoxin, exfoliative toxin A (ETA) (Toxin Technology) was added at 0.5 ug/ml for over 2 h to disrupt DSG1. Cells were washed with HBSS twice, and incubated with Dispase (Roche Diagnostics) for 30 min to detach the monolayer sheets. The detached cells were further mechanically dissociated by pipetting. After pipetting, the cells were observed by light microscopy.

AK23 antibody, which was derived from an active PV mouse model (*27*) and is known to inhibit cell–cell interaction, was used as the positive control for this assay.

Mouse IgG2a mAb AK23m was generated by a similar process to 18-1m, using a published sequence of the variable region of mAb AK23, which induces PV (*19*, *28*).

Determination of ADCC

ADCC activity of mAbs was determined as follows. Tumour cells were cultured in RPMI1640 with penicillin/streptomycin and 10% FBS (RPMI medium). About 1×10^6 cell of mouse DSG3/BaF3 or human DSG3/BaF3 was suspended in 200 μl of RPMI medium with 3.7 MBq of ^{51}Cr-sodium chromate (GE Healthcare) and incubated in 5% CO_2, at 37°C for 1 h. Cells were washed with RPMI medium adjusted to a concentration of 2×10^5 cells/ml and dispensed at 50 μl into a 96-well U-bottomed plate. Then 50 μl of antibody solution was added to each well, and the plates were incubated for 15 min at room temperature. Next 5×10^4 cells of mFcγRIIIa-NK92 (in the case of mouse IgG2a chimeric antibodies) or NK92 (in the case of human IgG1 chimeric antibodies) were added as effector cells. The tumour cells were further incubated at 37°C for 4 h in 5% CO_2. 100 μl of supernatants were collected from each well and radioactivity in the supernatants was measured with a gamma counter (1480 WIZARD 3″, Wallac). ^{51}Cr release was calculated based on the following formula:

$$\text{Specific } {}^{51}\text{Crrelease } (\%) = (A - C)/(B - C) \times 100$$

where A is the ^{51}Cr release of each well (cpm), B is the mean ^{51}Cr release for 50 μl of cells incubated in 150 μl of 2% Nonidet P-40 (Nakalai Tesque) and C is the mean ^{51}Cr release for 50 μl of cells incubated in 150 μl of RPMI medium (cpm). All experiments were conducted in duplicate. Median value and standard deviation were calculated. Mouse IgG2a (Becton Dickinson) was used as a negative control antibody.

Determination of anti-tumour efficacy and toxicity *in vivo*

The anti-tumour activity of anti-mouse DGS3 antibodies was evaluated using a syngeneic mouse model as follows. Balb/c mice were inoculated subcutaneously with approximate 3 mm^3 cubes of LC-12 tumour tissue. Mice were divided into three groups one day after tumour inoculation. Each group consisted of 10 mice, and 18-1m, df-18-1m (10 mg/kg) or vehicle (PBS) was administered intravenously on days 1, 8 and 15. Tumour volume and body weight were measured twice a week.

Anti-tumour efficacy and toxicity were evaluated in human SCC xenograft models. About 1×10^7 cells of HARA and A431 cells suspended in HBSS were inoculated and approximate 3 mm^3 cubes of SCC-15 tumour tissue were inoculated subcutaneously into SCID mice. When the mean tumour volumes reached 100 mm^3, 80 mm^3 and 120 mm^3, respectively, the mice were subjected to the study. Seven and five SCID mice per group (HARA and A431) were dosed intravenously with 10 mg/kg of mAb (df-DF366m) or with vehicle (PBS) once a week. Four SCID mice per group (SCC-15) were dosed intraperitoneally with 10 mg/kg of mAb (df-DF366m) or vehicle (PBS) once a week for 5 weeks. Tumour volume and body weight were measured twice a week. Tumour volume was determined with the formula: $ab^2/2$ (mm^3), where a and b are the longest and shortest diameters, respectively. Statistical analysis was conducted with the Dunnett's test (LC-12) and t-test (HARA, A431 and SCC-15) using the SAS statistical package software (SAS Institute). Statistical significance was judged at $P < 0.05$.

At necropsy, the animals were euthanized by exsanguination from the abdominal artery under deep isoflurane anaesthesia. The small intestine, colon, liver, kidney, spleen and thymus, and tissues with squamous epithelia (skin, oral mucosa, oesophagus and forestomach) were fixed in 10% neutral-buffered formalin, and embedded into paraffin by a routine method. Thin sections were prepared at a

thickness of 5 μm, stained with haematoxylin and eosin, and read under a light microscope. Inflammatory cell infiltration was evaluated pathologically by certified pathologists.

Results

DSG3 expression in human tissues

Six out of six cases of SCC in various organs were positive for DSG3 (Fig. 1A). The staining of a representative sample is shown in Fig. 1B (left panel). In 5/6 cases, the staining score was higher than 200, and two of the lung SCC cases had scores higher than 300. In contrast, only 1/6 cases was positive for adenocarcinoma in the lung, and the score was notably lower than lung SCC. In non-cancerous tissue, the epidermis in tumour adjacent skin was positive in 2/2 cases (Fig. 1A). DSG3 expression was observed from the basal cell layer to prickle cell layer (Fig. 1B, right panel). Epidermal hyperplasia was present, but the staining score was lower than 200 and tended to be lower compared with SCC.

Generation of anti-mouse DSG3 mAbs with ADCC activity

To confirm the proof of concept in non-clinical models, we attempted to generate an anti-mouse DSG3 mAb that has anti-tumour activity by ADCC to SCC, but with no cell–cell dissociating effects in keratinocytes that cause PV (Fig. 2A).

By FACS with hybridoma supernatants, 34 clones with robust binding activity were selected. Next, ADCC activity was measured with an antibody concentration of 1 μg/ml, and 12 clones with the strongest ADCC activity were further selected (Fig. 2B).

Selection of clones with no PV-like effects by evaluation of Ca^{2+}-dependent binding and the cell–cell dissociation assay

The above-mentioned 12 clones were examined for Ca^{2+}-dependent binding to mouse DSG3 by FACS. As it is well-known that pathogenic anti-DSG3 antibodies like AK23 recognize an epitope with a calcium-dependent conformation, we screened the antibodies for calcium dependency (*28*, *33*). Three clones, 18-1, 37-1 and 40-2, bound to mouse DSG3 equally with and without Ca^{2+}, and were determined as having Ca^{2+} independent binding activity (Fig. 2C). Other clones bound weakly to mouse DSG3 when Ca^{2+} was not present, and were determined as having Ca^{2+}-dependent binding activity.

Of the three clones with Ca^{2+} independent binding activity, clone 18-1 had the highest affinity, and so was selected for further evaluation. In order to ascertain the potential to induce PV, cell–cell dissociating activity in a mouse keratinocyte sheet was tested. The test was designed to compare the cellular effects induced by a difference only in antigen binding while the Fc function remained the same.

18-1 and AK23 were genetically engineered into mouse IgG2a-type chimeric antibodies 18-1m and AK23m, and were subjected to the assay. 18-1m did not induce keratinocyte dissociation, while the positive control antibody AK23m did. This was thought to show that 18-1m was not pathogenic (Fig. 2D).

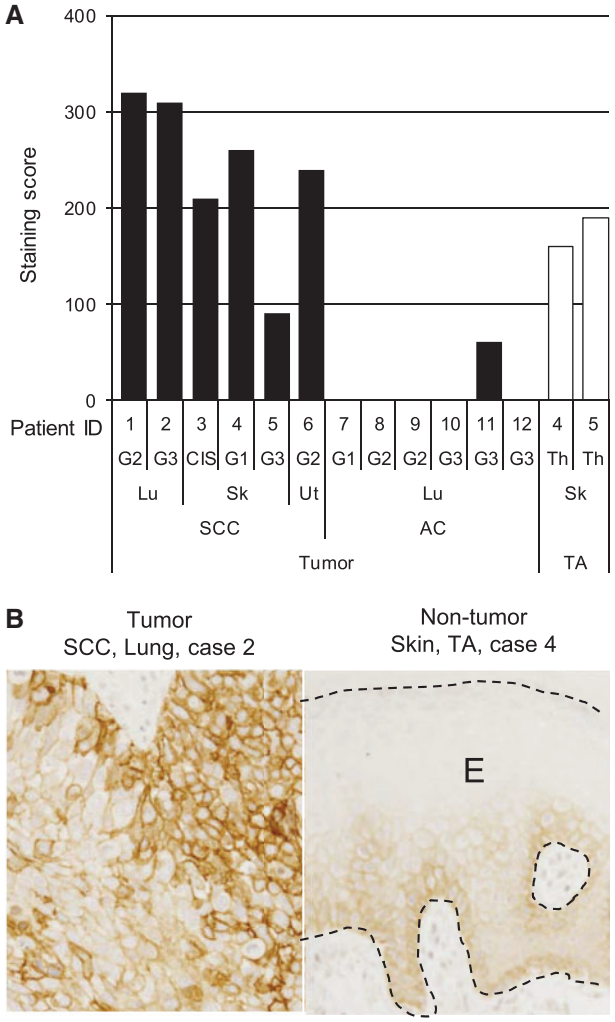

Fig. 1 Expression of DSG3 in human tissues. (**A**) DSG3 was expressed frequently in SCC of various organs compared with adenocarcinoma of the lung. Tumour-adjacent skin also expressed DSG3. G1–G3, histology grade; CIS, carcinoma *in situ*; Th, thickening of epidermis; SCC, squamous cell carcinoma; AC, adenocarcinoma; TA, tumour-adjacent tissue; Lu, lung; Sk, skin; Ut, uterus. (**B**) Images of IHC staining in SCC of the lung (left panel) and tumour-adjacent skin (right panel). Labelled streptavidin-biotin method. E presents epidermis. Bar = 100 μm.

Enhancement of ADCC activity by defucosylation of antibody

As reported previously, an antibody produced by GFT (-/-) CHO cells is mainly a fucose-free oligosaccharide (*7*), a so-called defucosylated antibody, which binds strongly to mouse FcγRIIIa and thus exhibits much enhanced ADCC. A defucosylated antibody, df-18-1m, induced ADCC activity that was comparable to a 10-fold concentration of 18-1m. Thus we confirmed that defucosylation further enhanced ADCC (Fig. 2E).

Anti-tumour efficacy and toxicity of 18-1m, df-18-1m antibodies in vivo

As we were able to generate an anti-mouse DSG3 antibody with the potential of anti-tumour ADCC activity but no pathogenic activity to normal tissues, we examined the proof of concept in a syngeneic mouse model of a mouse lung SCC cell line, LC12.

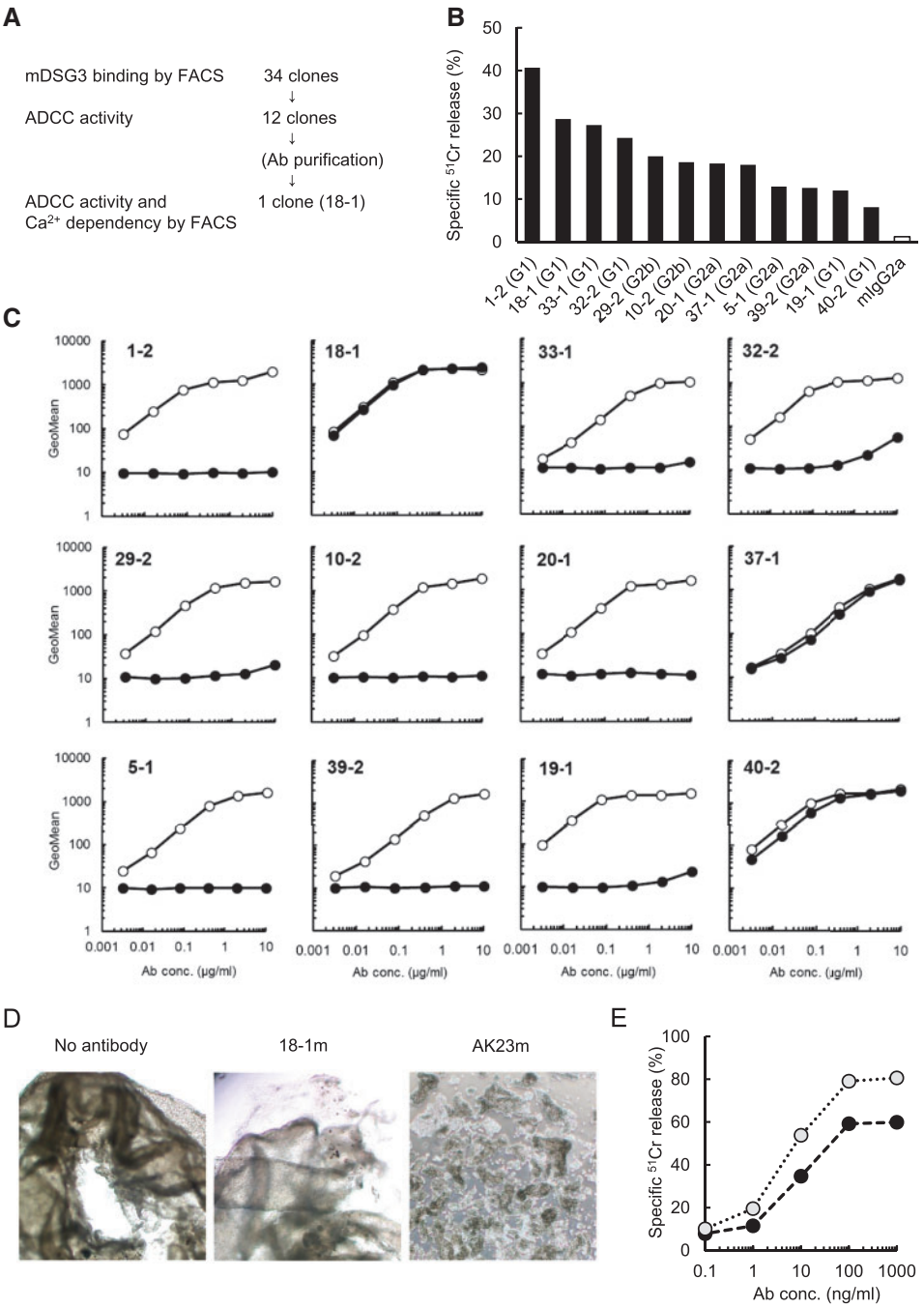

Fig. 2 Characterization of anti-mouse DSG3 mAbs. (**A**) Screening flow for an anti-mouse DSG3 mAb. (**B**) Analysis of ADCC activity. ^{51}Cr-labelled 1×10^4 mouse DSG3/BaF3 cells were incubated with hybridoma supernatant at 1 μg/ml antibody for 15 min. mFcγRIIIa-NK92 were added at E/T ratio = 5:1 and the cell suspensions were further incubated at 37°C for 4 h. The radioactivity was measured with Gamma counter. Specific ^{51}Cr release was calculated. Mouse IgG2a was used as reference control. (**C**) Analysis of Ca^{2+}-dependent binding activity to mouse DSG3. Serial diluted mAbs were incubated with mouse DSG3/DG44. The binding activity to mouse DSG3 was measured with FACS with EDTA (closed circle) or without EDTA (open circle). (**D**) Analysis of cell–cell dissociating activity with mouse IgG2a type chimeric anti-DSG3 18-1m. Cell–cell dissociating activity with mAb 18-1m was analysed by keratinocyte dissociation assay (*27*). mAb AK23m was used as positive control. (**E**) ADCC enhancement by defucosylated chimeric anti-DSG3. ADCC activity of 18-1m was compared. Mouse DSG3/DG44 was incubated with serial diluted antibody and mixed with mFcγRIIIa-NK92 as effector cells. ADCC activity was measured. Black circle: 18-1m, grey circle: df-18-1m prepared with GFT (-/-) CHO cells.

After administering 18-1m or df-18-1m once a week for 3 weeks to LC12-inoculated mice, the body weight of antibody-administered mice was slightly lower compared with that of vehicle-administered mice at the end of the study. However, there were no changes in the general condition of mice in any of the groups and there is no serious toxicity (Fig. 3A).

In contrast, the tumour volume was significantly lower antibody-administered groups compared with the control group (Fig. 3B). Suppression of tumour

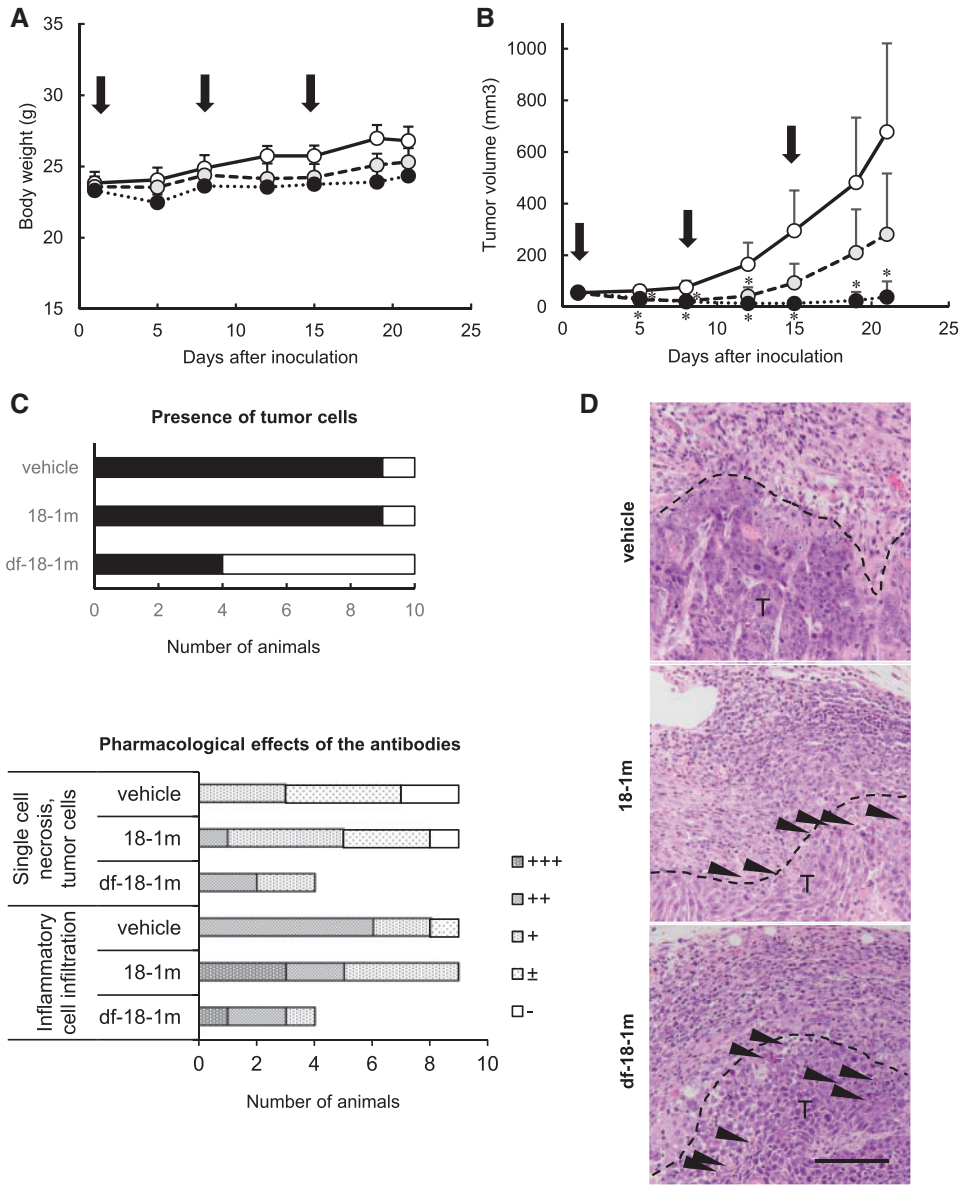

Fig. 3 Results of anti-mouse DSG3 mAb administration in tumour-bearing Balb/c mice. Anti-mouse DSG3 mAb 18-1m and df-18-1m were inoculated at 10 mg/kg in LC12 syngeneic mouse model. Days of treatment with mAb are shown by arrows. (**A**) Body weight change. (**B**) Tumour volume change. The mean for each group is shown for each time point. Bars indicate standard deviation of the mean. White circle, control; grey circle, 18-1m; black circle, df-18-1m. $*P<0.05$, compared with vehicle. (**C**) Histological examination of engrafted LC12 tumours. The presence of tumour cells in the site of engraftment (upper left). Closed square, present; open square, absent. Changes related to the pharmacological effects of the antibodies (lower left) are shown by severity of change: ±, very slight; +, slight; ++, moderate; +++, severe. (**D**) Representative images of tumours in each group. Increased inflammatory cell infiltration and single-cell necrosis (arrow heads) were observed in antibody administered tumours. The changes were noted around the interface (broken line) of the tumour mass (T) with surrounding tissue. Bar = 100 μm.

growth was marked in the df-18-1 group compared with the 18-1m group. The number of cases with tumour volumes of less than 3 mm^3 or with no palpable mass of histologically detectable tumour cells was 1/10 in each of the control and 18-1m groups, but 6/10 in the df-18-1m group (Fig. 3C). Histopathologically, single-cell necrosis of tumour cells and inflammatory cell infiltration were observed in palpable tumours of the 18-1m group. Similar changes were observed in the palpable tumours of the df-18-1m group (Fig. 3C and D).

There were no histopathological changes in tissues containing squamous cells (skin, oral mucosa, oesophagus and forestomach) and other tissues (intestine, colon, liver, kidney, spleen and thymus).

Generation of anti-human DSG3 antibody

The results from the mouse studies showed the possibility that antibodies with anti-tumour activity and no PV-like pathogenic activity could be generated, so we proceeded to generate an anti-human DSG3 antibody with similar features.

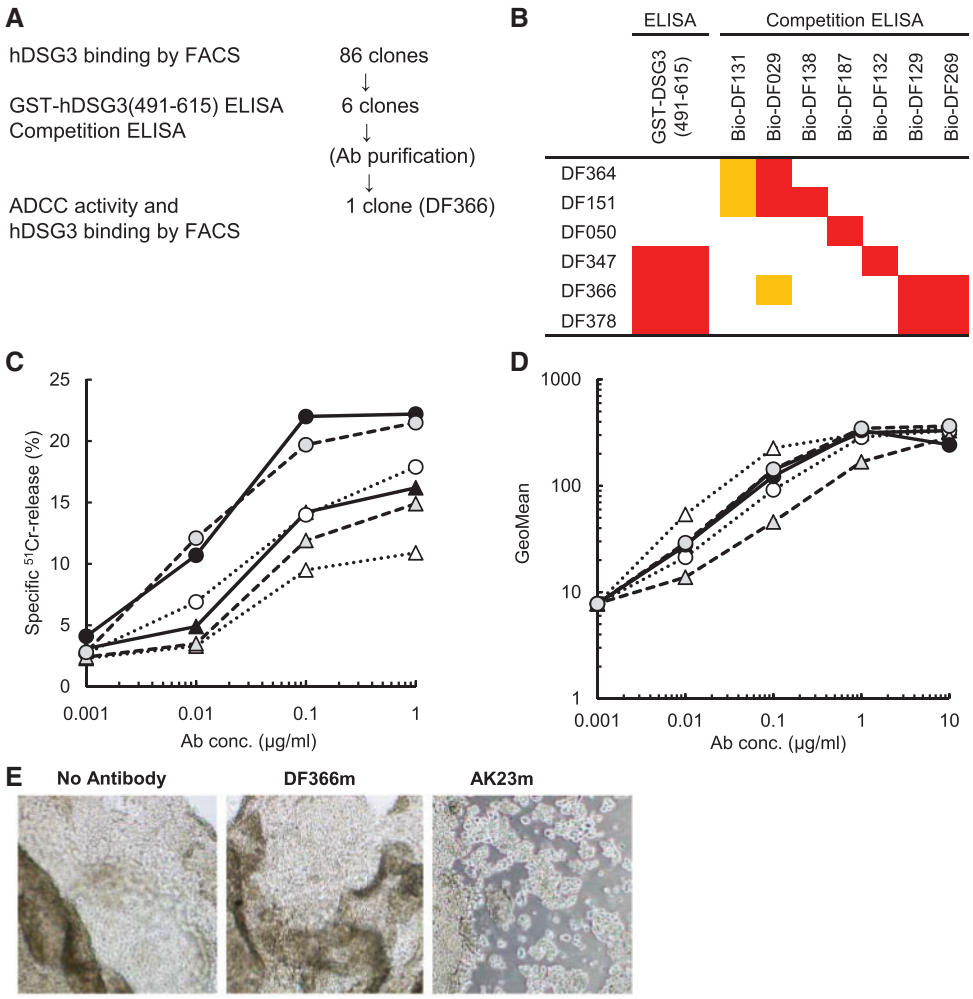

Fig. 4 Characterization of anti-human DSG3 mAbs. (**A**) Screening flow for an anti-human DSG3 mAb. (**B**) Classification of mAbs with GST-human DSG3 (aa 491-615) ELISA and competition ELISA. In GST-ELISA, dark grey indicates positive. In competition ELISA, dark grey indicates >90% inhibition and light grey indicates >70% inhibition. Bio-(antibody number) indicates a biotinylated antibody. (**C**) ADCC activity was measured as specific ^{51}Cr release. Black circle, DF366c; grey circle, DF378c; white circle, DF347c; black triangle, DF151c; grey triangle, DF364c; white triangle, DF050c. (**D**) Binding activity to human DSG3/DG44. Serial diluted antibody was incubated with human DSG3/DG44, and binding activity was measured with FACS. Symbols are the same as (C). (**E**) Cell–cell dissociation activity was analysed in human keratinocytes. Mouse IgG2a chimeric antibody DF366m was compared with AK23m as a positive control.

The screening flow in Fig. 4A shows how the antibody was selected. We immunized mice with human sDSG3-mIgG2aFc protein, and established 86 hybridoma clones that were positive for activity against human DSG3, from which clones with high affinity were selected by FACS. In general, the epitopes that are contained in the membrane-proximal region of a membrane protein tend to give high ADCC (*26*, *31*), so hDSG3 (aa 491-615, which is equivalent to the membrane-proximal region) would be a candidate for an ADCC epitope. Therefore, we added a GST-DSG3 ELISA to the screening to obtain an antibody that would bind to a region that is safely distant from the EC1-EC2 domains and would have higher ADCC.

To select clones that bound to a unique binding region, we used a competition ELISA in the following procedure. First, seven of the hybridoma clones that gave no cross-reaction were chosen as competition antibodies and were biotinylated. Then, the competition ELISA divided the hybridoma clones into six groups, and a representative clone from each group was selected after evaluating the binding affinity by FACS and the ADCC. Chimeras of each of these clones were generated with a human IgG1 Fc portion to compare the cytotoxic effects in a clinically relevant format.

Figure 4B summarizes the characters of the six representative clones. Their ADCC was categorized into two levels of activity: high (two clones) and middle (four clones) (Fig. 4C). As expected, the binding regions of the two clones with the strongest ADCC, DF366 and DF378, were located between aa 491 and 615. There was no difference in binding affinity of the two clones with high ADCC (Fig. 4D).

From these results, DF366 was selected as the clone with strongest ADCC activity and converted to a mouse IgG2a subclass (designated as DF366m) to evaluate cell–cell dissociation activity in human

keratinocyte sheets. DF366m did not show cell–cell dissociation activity, while the positive control AK23m antibody did (Fig. 4E).

Anti-tumour efficacy of anti-human DSG3 mAbs against SCC

ADCC activity of DF366m was compared with a defucosylated antibody (df-DF366m) with mFcγRIIIa-NK92 as the effector cells. The anti-tumour effect of ADCC-enhanced df-DF366m was evaluated in an *in vitro* ADCC assay with human SCC cell lines HARA, A431 or SCC-15. The results showed that both DF366 and df-DF366m have ADCC activity against human SCC cell lines (Fig. 5A). df-DF366m showed strong ADCC activity even at concentrations that were several score times lower than DF366m.

Next, the anti-tumour effect of df-DF366m was investigated *in vivo* using xenograft models of HARA, A431 and SCC-15. In all models, efficacy of df-DF366m was significantly enhanced (Fig. 5B). Especially in SCC-15, the tumour growth was completely inhibited.

Discussion

DSG3 has been reported to be highly expressed in lung SCC both at mRNA and protein levels (*16*, *17*, *29*). We examined the expression of DSG3 in SCC by IHC and confirmed that the expression was high, which was consistent with the reported results, and thus we considered that DSG3 is a potential target for therapeutic antibodies against SCC. On the other hand, DSG3 is also expressed in normal squamous epithelium (*16*), and autoantibodies against DSG3 cause PV, an autoimmune disease that includes severe skin lesions, such as blistering (*30*). Tsunoda *et al*. have also shown that anti-DSG3 mAbs induced PV blisters in a passive transfer assay with neonatal mouse (*15*). Because of those results, we judged it necessary to avoid PV-like pathogenic activity if we selected DSG3 as a target for a therapeutic antibody. We generated anti-DSG3 mAbs to examine their potential as a therapeutic antibody.

It is well-known that therapeutic antibodies can induce biological effects by several mechanisms. To attack cancer cells, a variety of modes of action have been utilized: mAb with ADCC, CDC activity that utilizes the host immune response, toxin-conjugated antibodies that utilize antibodies as a drug delivery system and so on (*6*, *10*). The ADCC activity of an antibody is considered to be dependent on the amount of antigen available to induce host immune response and cytotoxicity (*7*, *31*, *32*). In this study, we have found that some SCC cases express higher levels of DSG3 than non-tumour. Thus we hypothesized that a mode of action via ADCC would be effective for obtaining tumour specificity.

In order to achieve our concept, it was thought necessary to generate an antibody with no PV-like pathogenic activity. It has been reported that in the pemphigus pathogenesis the neutralizing activity of patient pathogenic autoantibodies causes a disruption of the DSG3-DSG3 adhesive interaction, and that subsequently destroys the epithelial cell structure (*15*). It is also known that autoantibodies with a Ca^{2+}-sensitive epitope cause cell–cell dissociation, and that these antibodies recognize a Ca^{2+}-dependent conformation

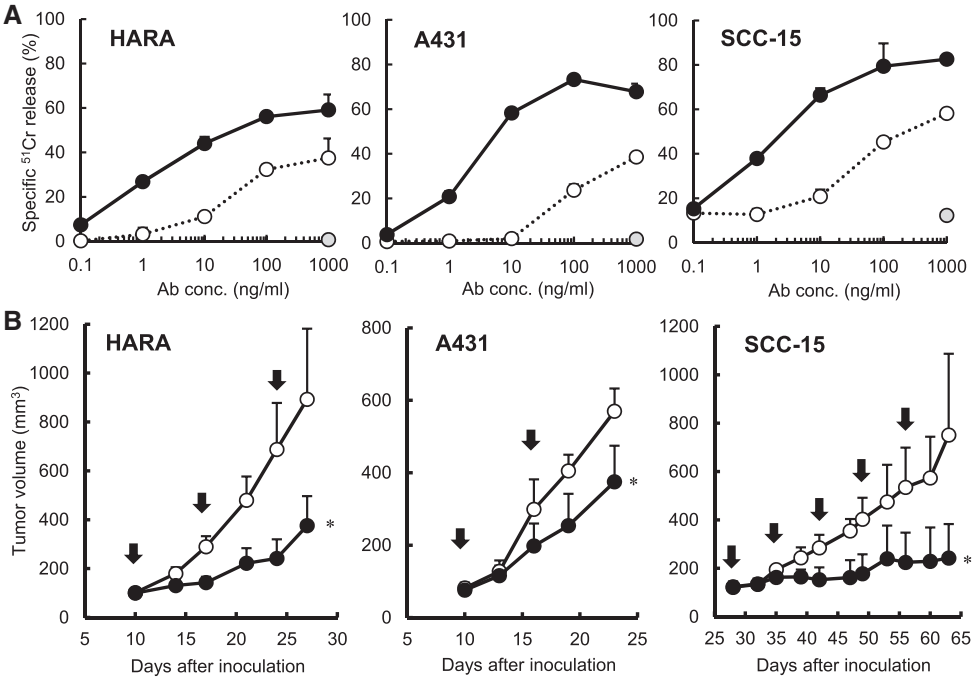

Fig. 5 Anti-tumour activity of defucosylated anti-human DSG3. (**A**) ADCC activity was measured with SCC cell lines. Bars indicate standard deviation of the mean. HARA, human lung SCC; A431, human skin SCC; SCC-15, human tongue SCC. DF366m (white circle), df-DF366m (black circle), control mIg2a (grey circle). (**B**) Each SCC cell line was inoculated s.c. in SCID mice. Mice were treated with mAb df-DF366m (black circle) or vehicle, PBS (white circle) on the days indicated by arrows. Tumour volume was measured twice a week. Bars indicate standard deviation of the mean. $*P<0.05$, compared with vehicle.

epitope that regulates cell–cell adhesion function (*33*). As epitope specificity is critical for PV activity, we considered it possible to add the ADCC function to an antibody while avoiding PV activity by selecting an appropriate epitope. Thus we attempted to obtain a wide variety of antibodies for functional screening.

In order to generate a wide variety of antibodies we utilized KO mice for immunization as described previously (*34*, *35*). Additionally we applied a DNA immunization method and were able to obtain a large number of different antibodies. Next, we adopted functional screening methods to select antibodies that have ADCC activity, but do not cause PV-like action. Conventional assay systems with mouse splenocytes are known to yield inconsistent results between lots, and the preparation is also a complicated process. Thus we established an ADCC screening system with the mFcγRIIIa-NK92 cell line that could stably measure ADCC activity. To screen for mAbs with no PV-like effects, we tested binding to DSG3 in a Ca^{2+} independent manner by ELISA and FACS in the presence of a Ca^{2+} chelating agent, EDTA. As a result we obtained anti-mouse DSG3 antibodies with ADCC activity *in vitro*, but no keratinocyte cell–cell dissociation.

We investigated the binding region of these clones by domain-swapped mutant analysis, and found that the mouse clone 18-1 binds to a region in the cadherin domains not EC1, while DF366 recognizes the membrane-proximal region (data not shown). When screening for anti-human DSG3 antibodies, we could not obtain antibodies that were cross-reactive to mouse DSG3. Mouse and human DSG3 are very homologous apart from their membrane-proximal regions, which tend to contain binding regions that provide high ADCC. When we screened for the anti-human DSG3 antibody, we aimed for an antibody that bound to a region that induced higher ADCC and was safely distant from the EC1-EC2 domains. With this in mind, we considered the best antibody against human DSG3 would be derived from a clone that bound to the proximal region. We therefore used a competition ELISA to classify the clones according to their binding regions and then selected the antibody in each group with the highest ADCC.

As ADCC activity and PV-like activity are different modes of action, we considered that enhancing ADCC would be an effective approach to improve anti-tumour activity without causing a toxic effect to the skin. To this end, we chose the mouse antibody that had the highest ADCC activity and enhanced its ADCC activity by changing to an IgG2a version (*36*, *37*) and a defucosylated version of the antibody using the GFT (-/-) CHO cells (*7*). Then, to test our hypothesis *in vivo*, we evaluated the non-defucosylated and defucosylated antibodies for anti-tumour activity and PV-like pathogenic activity in a mouse model. *In vivo* anti-tumour activity was observed with both antibodies, but the enhanced ADCC activity did not lead to additional weight loss or induction of severe toxicity, such as patchy hair loss, oral erosion and death, which are reported in mice dosed with PV-inducible anti-DSG3 AK23 (*38*). In a preliminary study with another mouse model, we observed minor, non-lethal changes in the vaginal mucosa, and we are currently studying the lesions in detail. From these results we judged that the defucosylated antibody improved anti-tumour activity, while the enhanced ADCC activity was not associated with enhanced toxicity. The current results in the mouse model strongly suggest that the neutralizing activity that disrupts DSG3 adhesive interaction can be separated from cytotoxicity by ADCC to DSG3-expressing cells. Therefore DSG3 was thought to be a suitable target for therapeutic antibody development.

Because the potential of DSG3 as a therapeutic target was shown in a mouse model, we attempted to generate an anti-human DSG3 antibody with similar characteristics to the mouse antibody. We succeeded in generating an antibody that binds to DSG3, with ADCC activity *in vitro*, and no adhesive interference activity to keratinocytes. Defucosylated anti-human DSG3 antibody showed anti-tumour activity against three differential SCC cell lines in xenograft models. These results indicate that it is possible to generate an anti-human DSG3 antibody with the same properties as our anti-mouse DSG3 antibody. It should be noted that effects in normal tissues could not be evaluated in mouse xenograft models with anti-human DSG3 antibody because the antibody does not recognize mouse DSG3. To address these issues, future toxicity studies will be necessary.

Ideally, therapeutic antibodies that function by cytotoxicity to cancer cells should target an antigen that is tumour-specific with no expression in normal tissues. However such tumour-specific antigens are very rare (*39*). Here we show it is possible to develop novel anti-tumour therapeutic antibodies even if the target molecule is expressed in both tumour and normal tissues, by carefully selecting the appropriate epitope and mode of action. Such an approach may enable currently undruggable targets to be targeted in the future.

Supplementary Data

Supplementary Data are available at *JB* Online.

Acknowledgements

We would like to express our thanks to Ms Kumiko Nakajima, Dr Yuichi Hirata, Dr Hirofumi Sakumoto, Dr Kenji Yoshida and Dr Naoki Kimura for the preparation of materials, Dr Kenji Adachi and Mr Takashi Nishizawa for their animal experiment assistance. Dr Tatsumi Yamazaki gave us constructive comments and warm encouragement. We also thank Sally Matsuura for proofreading the manuscript.

Conflict of Interest

The authors S.F., S.K., E.F. and K.N. are employees of Forerunner Pharma Research Co., Ltd. founded by Chugai Pharmaceutical Co., Ltd., and the authors E.F., K.T. and M.S. are employees of Chugai Pharmaceutical Co., Ltd. They declare no other potential conflict of interest.

References

1. Weiner, L.M., Dhodapkar, M.V., and Ferrone, S. (2009) Monoclonal antibodies for cancer immunotherapy. *Lancet* **373**, 1033–1040

2. Rajasekaran, N., Chester, C., Yonezawa, A., Zhao, X., and Kohrt, H.E. (2015) Enhancement of antibody-dependent cell mediated cytotoxicity: a new era in cancer treatment. *Immunotargets Ther*. **4**, 91–100
3. Shuptrine, C.W., Surana, R., and Weiner, L.M. (2012) Monoclonal antibodies for the treatment of cancer. *Semin. Cancer Biol*. **22**, 3–13
4. Mauerer, R. and Gruber, R. (2012) Monoclonal antibodies for the immunotherapy of solid tumours. *Curr. Pharm. Biotechnol*. **13**, 1385–1398
5. Kohrt, H.E., Houot, R., Marabelle, A., Cho, H.J., Osman, K., Goldstein, M., Levy, R., and Brody, J. (2012) Combination strategies to enhance antitumor ADCC. *Immunotherapy* **4**, 511–527
6. Suzuki, M., Kato, C., and Kato, A. (2015) Therapeutic antibodies: their mechanisms of action and the pathological findings they induce in toxicity studies. *J. Toxicol. Pathol*. **28**, 133–139
7. Ishiguro, T., Kawai, S., Habu, K., Sugimoto, M., Shiraiwa, H., Iijima, S., Ozaki, S., Matsumoto, T., and Yamada-Okabe, H. (2010) A defucosylated anti-CD317 antibody exhibited enhanced antibody-dependent cellular cytotoxicity against primary myeloma cells in the presence of effectors from patients. *Cancer Sci*. **101**, 2227–2233
8. Nakano, K., Ishiguro, T., Konishi, H., Tanaka, M., Sugimoto, M., Sugo, I., Igawa, T., Tsunoda, H., Kinoshita, Y., Habu, K., Orita, T., Tsuchiya, M., Hattori, K., and Yamada-Okabe, H. (2010) Generation of a humanized anti-glypican 3 antibody by CDR grafting and stability optimization. *Anti-cancer Drugs* **21**, 907–916
9. Harada, T., Ozaki, S., Oda, A., Tsuji, D., Ikegame, A., Iwasa, M., Udaka, K., Fujii, S., Nakamura, S., Miki, H., Kagawa, K., Kuroda, Y., Kawai, S., Itoh, K., Yamada-Okabe, H., Matsumoto, T., and Abe, M. (2013) Combination with a defucosylated anti-HM1.24 monoclonal antibody plus lenalidomide induces marked ADCC against myeloma cells and their progenitors. *PLoS One* **8**, e83905
10. Weiner, G.J. (2015) Building better monoclonal antibody-based therapeutics. *Nat. Rev. Cancer* **15**, 361–370
11. Savci-Heijink, C.D., Kosari, F., Aubry, M.C., Caron, B.L., Sun, Z., Yang, P., and Vasmatzis, G. (2009) The role of desmoglein-3 in the diagnosis of squamous cell carcinoma of the lung. *Am. J. Pathol*. **174**, 1629–1637
12. Zhan, C., Yan, L., Wang, L., Sun, Y., Wang, X., Lin, Z., Zhang, Y., Shi, Y., Jiang, W., and Wang, Q. (2015) Identification of immunohistochemical markers for distinguishing lung adenocarcinoma from squamous cell carcinoma. *J. Thorac. Dis*. **7**, 1398–1405
13. Xin, Z., Yamaguchi, A., and Sakamoto, K. (2014) Aberrant expression and altered cellular localization of desmosomal and hemidesmosomal proteins are associated with aggressive clinicopathological features of oral squamous cell carcinoma. *Virchows Arch. Pathol*. **465**, 35–47
14. Fang, W.-K., Chen, B., Xu, X.-E., Liao, L.-D., Wu, Z.-Y., Wu, J.-Y., Shen, J., Xu, L.-Y., and Li, E.-M. (2014) Altered expression and localization of desmoglein 3 in esophageal squamous cell carcinoma. *Acta Histochem*. **116**, 803–809
15. Stanley, J.R. and Amagai, M. (2006) Pemphigus, bullous impetigo, and the staphylococcal scalded-skin syndrome. *N. Engl. J. Med*. **355**, 1800–1810
16. Zenzo, G., Di Amber, K.T., Sayar, B.S., Muller, E.J., and Borradori, L. (2016) Immune response in pemphigus and beyond: progresses and emerging concepts. *Semin. Immunopathol*. **38**, 57–74
17. Di Zenzo, G., Di Lullo, G., Corti, D., Calabresi, V., Sinistro, A., Vanzetta, F., Didona, B., Cianchini, G., Hertl, M., Eming, R., Amagai, M., Ohyama, B., Hashimoto, T., Sloostra, J., Sallusto, F., Zambruno, G., and Lanzavecchia, A. (2012) Pemphigus autoantibodies generated through somatic mutations target the desmoglein-3 cis-interface. *J. Clin. Invest*. **122**, 3781–3790
18. Heupel, W.M., Zillikens, D., Drenckhahn, D., and Waschke, J. (2008) Pemphigus vulgaris IgG directly inhibit desmoglein 3-mediated transinteraction. *J. Immunol*. **181**, 1825–1834
19. Tsunoda, K., Ota, T., Aoki, M., Yamada, T., Nagai, T., Nakagawa, T., Koyasu, S., Nishikawa, T., and Amagai, M. (2003) Induction of pemphigus phenotype by a mouse monoclonal antibody against the amino-terminal adhesive interface of desmoglein 3. *J. Immunol*. **170**, 2170–2178
20. Fujii, E., Suzuki, M., Matsubara, K., Watanabe, M., Chen, Y.J., Adachi, K., Ohnishi, Y., Tanigawa, M., Tsuchiya, M., and Tamaoki, N. (2008) Establishment and charactrizatio of *in vivo* human tumor models in the NOD/SCID/γ_c^{null} mouse. *Pathol. Int*. **58**, 559–567
21. Sato, Y., Mukai, K., Watanabe, S., Goto, M., and Shimosato, Y. (1986) The AMeX method. A simplified technique of tissue processing and paraffin embedding with improved preservation of antigens for immunostaining. *Am. J. Pathol*. **125**, 431–435
22. Suzuki, M., Katsuyama, K., Adachi, K., Ogawa, Y., Yorozu, K., Fujii, E., Misawa, Y., and Sugimoto, T. (2002) Combination of fixation using PLP fixative and embedding in paraffin by the AMeX method is useful for histochemical studies in assessment of immunotoxicity. *J. Toxicol. Sci*. **27**, 165–172
23. Kohler, G. and Milstein, C. (1975) Continous culture of fused cells escreting antibody of predefined specificity. *Nature* **256**, 495–497
24. Tang, Y., Lou, J., Alpaugh, R.K., Robinson, M.K., Marks, J.D., and Weiner, L.M. (2007) Regulation of antibody-dependent cellular cytotoxicity by IgG intrinsic and apparent affinity for target antigen. *J. Immunol*. **179**, 2815–2823
25. VanAntwerp, J.J. and Wittrup, K.D. (2000) Fine affinity discrimination by yeast surface display and flow cytometry. *Biotechnol. Prog*. **16**, 31–37
26. Nakano, K., Orita, T., Nezu, J., Yoshino, T., Ohizumi, I., Sugimoto, M., Furugaki, K., Kinoshita, Y., Ishiguro, T., Hamakubo, T., Kodama, T., Aburatani, H., Yamada-Okabe, H., and Tsuchiya, M. (2009) Anti-glypican 3 antibodies cause ADCC against human hepatocellular carcinoma cells. *Biochem. Biophys. Res. Commun*. **378**, 279–284
27. Ishii, K., Harada, R., Matsuo, I., Shirakata, Y., Hashimoto, K., and Amagai, M. (2005) *In vitro* keratinocyte dissociation assay for evaluation of the pathogenicity of anti-desmoglein 3 IgG autoantibodies in pemphigus vulgaris. *J. Investig. Dermatol*. **124**, 939–946
28. Tsunoda, K., Amagai, M., Nishikawa, T., and Koyasu, S. (2003) Pemphigus monoclonal antibody. WO2003020769.
29. Inamura, K., Fujiwara, T., Hoshida, Y., Isagawa, T., Jones, M.H., Virtanen, C., Shimane, M., Satoh, Y., Okumura, S., Nakagawa, K., Tsuchiya, E., Ishikawa, S., Aburatani, H., Nomura, H., and Ishikawa, Y. (2005) Two subclasses of lung squamous cell carcinoma with different gene expression profiles and prognosis

identified by hierarchical clustering and non-negative matrix factorization. *Oncogene* **24**, 7105–7113

30. Amagai, M., Klaus-Kovtun, V., and Stanley, J.R. (1991) Autoantibodies against a novel epithelial cadherin in pemphigus vulgaris, a disease of cell adhesion. *Cell* **67**, 869–877
31. Kawai, S., Koishihara, Y., Iida, S., Ozaki, S., Matsumoto, T., Kosaka, M., and Yamada-Okabe, H. (2006) Construction of a conventional non-radioisotope method to quantify HM1.24 antigens: correlation of HM1.24 levels and ADCC activity of the humanized antibody against HM1.24. *Leuk. Res.* **30**, 949–956
32. Kawai, S., Yoshimura, Y., Iida, S., Kinoshita, Y., Koishihara, Y., Ozaki, S., Matsumoto, T., Kosaka, M., and Yamada-Okabe, H. (2006) Antitumor activity of humanized monoclonal antibody against HM1.24 antigen in human myeloma xenograft models. *Oncol. Rep.* **15**, 361–367
33. Amagai, M., Ishii, K., Hashimoto, T., Gamou, S., Shimizu, N., and Nishikawa, T. (1995) Conformational epitopes of pemphigus antigens (Dsg1 and Dsg3) are calcium dependent and glycosylation independent. *J. Invest. Dermatol.* **105**, 243–247
34. Saitoh, R., Ohtomo, T., Yamada, Y., Kamada, N., Nezu, J., Kimura, N., Funahashi, S., Furugaki, K., Yoshino, T., Kawase, Y., Kato, A., Ueda, O., Jishage, K., Suzuki, M., Fukuda, R., Arai, M., Iwanari, H., Takahashi, K., Sakihama, T., Ohizumi, I., Kodama, T., Tsuchiya, M., and Hamakubo, T. (2007) Viral envelope protein gp64 transgenic mouse facilitates the generation of monoclonal antibodies against exogenous membrane proteins displayed on baculovirus. *J. Immunol. Methods* **322**, 104–117
35. Hamakubo, T., Arai, O., and Iwanari, H. (2014) Generation of antibodies against membrane proteins. *Biochim. Biophys. Acta* **1844**, 1920–1924
36. Herlyn, D., Herlyn, M., Steplewski, Z., and Koprowski, H. (1985) Monoclonal anti-human tumor antibodies of six isotypes in cytotoxic reactions with human and murine effector cells. *Cell. Immunol.* **92**, 105–114
37. Kipps, T.J., Parham, P., Punt, J., and Herzenberg, L.A. (1985) Importance of immunoglobulin isotype in human antibody-dependent, cell-mediated cytotoxicity directed by murine monoclonal antibodies. *J. Exp Med.* **161**, 1–17
38. Tsunoda, K., Ota, T., Saito, M., Hata, T., Shimizu, A., Ishiko, A., Yamada, T., Nakagawa, T., Kowalczyk, A.P., and Amagai, M. (2011) Pathogenic relevance of IgG and IgM antibodies against desmoglein 3 in blister formation in pemphigus vulgaris. *Am. J. Pathol.* **179**, 795–806
39. Shim, H. (2011) One target, different effects: a comparison of distinct therapeutic antibodies against the same targets. *Exp. Mol. Med.* **43**, 539–549